Alma Mater Studiorum - Università di Bologna

SCUOLA DI SCIENZE

Dipartimento di Chimica Industriale “Toso Montanari”

Corso di Laurea Magistrale in

Chimica Industriale

Classe LM-71 - Scienze e Tecnologie della Chimica Industriale

Synthesis of new non-fullerene acceptors based on indacenodithiophene core for organic solar cells

Tesi di laurea sperimentale

CANDIDATO

Alice Nanni

RELATORE

Prof.ssa Carla Boga

CORRELATORI

Prof. Iain McCulloch

Prof. Massimiliano Lanzi

Anno Accademico 2018-2019

Abstract

Due to the low cost, lightness and flexibility, Polymer Solar Cell (PSC) technology is considered one of the most promising energy technologies. In the past decades, PSCs using fullerenes or fullerene derivatives as the electron acceptors have made great progress with best power conversion efficiency (PCE) reaching 11%. However, fullerene type electron acceptors have several drawbacks such as complicated synthesis, a low light absorption coefficient and poor tuning in energy levels, which prevent the further development of fullerene-based PSCs. Hence the need to have a new class of electron acceptors as an alternative to conventional fullerene compounds. Non-fullerene acceptors (NFAs) have developed rapidly in the last years and the maximum PCEs have exceeded 14% for single-junction cells and 17% for double-junction tandem cells. By combining an electron-donating backbone, generally with several fused rings with electron-withdrawing units, we can simply construct NFA of the acceptor–donor–acceptor type (A–D–A). Versatile molecular structures have been developed using methods such as acceptor motif engineering and donor motif engineering. However, there are only a few electron-donating backbones that have been proved to be successful. Therefore, it is still necessary to develop promising building blocks to further enrich the structural diversity. An indacenodithiophene (IDT) unit with just five fused rings has a sufficiently rigid coplanar structure, which has been regarded as one of the promising electron-rich units to design high-performance A–D–A NFAs. In this work, performed at the King Abdullah University of Science and Technology in Saudi Arabia, a new nine-cyclic building block (TBIDT) with a two benzothiophene unit was synthesized and used for designing new non-fullerene electron acceptors.

Table of contents

Abbreviations and acronyms list

PSC : Polymer Solar Cell

OSCs : Organic Solar Cells

NFAs : Non-Fullerene Acceptors

IDT : Indacenodithiophene

HOMO : Highest occupied molecular orbital

LUMO : Lowest unoccupied molecular orbital

E_C : Conductive band

E_V : Valence band

E_{GAP} : Energy gap

E_{PH} : Energy of the photon

EQE : External Quantum Efficiency

IQE : Internal Quantum Efficiency

PCE : Power Conversion Efficiency

P_{IN} : Power irradiating the solar cell

P_{OUT} : maximum power at the output

V_{MPP} : Voltage at the Maximum Power Point (MMP)

J_{MPP} : Current at the Maximum Power Point (MPP)

J_{SC} : short-circuit current

V_{OC} : open-circuit voltage

FF : Fill Factor

q : elementary charge

BHJ : Bulk heterojunction solar cell

BT : 2,1,3-benzothiadiazole

TB : benzothiophene

PVCs : Photovoltaic cells

CIS : Cupper Indium Selenide

CIGS : Cupper Indium Gallium Selenide

DSSCs : Dye-Sensitized Solar Cells

ITO : Indium Tin Oxide

SCMs : Semiconducting Materials

NF-OSCs : Non-Fullerene Organic Solar Cells

IDTT : Indacenodithieno[3,2-b]thiophene

1. Introduction

Electricity undoubtedly had an impact in thriving the development of human civilisations. It is often linked to the overall living standard of a country whereby the higher the electricity consumption usually equates to an overall higher living standard and a more developed country. Currently, the demand of electricity in the world is met predominantly by non-renewable means. The fossil energy sources, ranging from the combustion of fossil fuels *i.e.* coal, petroleum, natural gas, are the major sources.

1.1. Issue with fossil fuels

Non-renewable energy sources such as fossil fuels[1] had thrived the economy of the world during the industrial revolution. As we know, the reserves of fossil energy sources are limited and burning leads to the emission of CO_2 and other pollutant chemicals which cause an increase of the greenhouse gases and lead to acceleration of global warming. The continual increase in using non-renewable sources of energy will undoubtedly have a negative impact in the overall ecological cycle of the world.

Therefore, the development of clean and renewable energy sources has become one of the major scientific and technological topics of the 21st century and clean, green and sustainable solar energy is one of these sources.

1.2. Awareness of switching energy sources

As shown in Figure 1, green renewable sources[2,3] of energy are on the rise and they are projected to be the major source of electricity in the future. This is simply an indication of the awareness in mankind regarding the unsustainability of the non-renewable sources of energy. Amongst all the renewable sources of energy, wind (which is harvested by a wind turbine) and solar (which is harvested by photovoltaic cells, generally) are projected to be the leaders in this matter.

The main issues with wind turbines are the size required to generate feasible amount of electricity, the noise that may affect the inhabitants in surrounding area and the destruction of flora and fauna whilst building one. Photovoltaic cells on the other hand do not possess such issue, as they are relatively smaller when compared to a wind turbine.

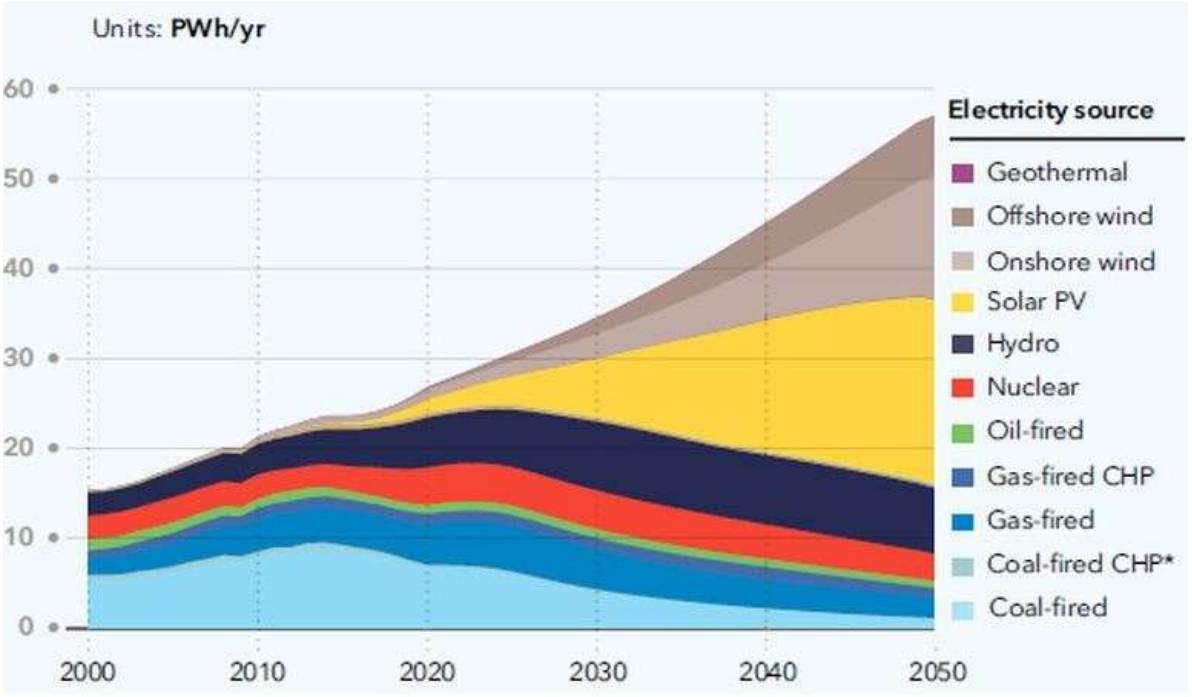

Figure 1: World electricity generation by source. Taken from DNV GL's Energy Transition Outlook.

1.3. Solar energy as the source of electricity

Solar radiation is arguably one of the most abundant sources of renewable energy available as it covers about 71% of the surface of the earth. The energy from the solar radiation can be harvested by photovoltaic effect[4]. It was in the 1839 that a French physicist A.E. Becquerel discovered that electricity could be produced directly from the sun radiation by applying photovoltaic effect. This effect is found in semiconductor materials, characterized by their intermediate properties in electrical conductivity between a conductor and an insulator. When the incident radiation in the form of photons reaches the material, electrons exist in the valence band are excited resulting in higher energy content. If the electrons acquire sufficient energy, they can be promoted to the conduction band and circulate through the material. This electron flow generates electric potential and upon application of an electric field on the semiconductor, the electrons move in the direction of the field, generating an electrical current.

1.4. Photovoltaic cells

Photovoltaic cells[5] (PVCs) are devices that convert solar radiation into electrical energy through the photovoltaic effect. The PVCs present an architecture based on the union of two semiconductor regions with different electron concentration. These materials can be type-n (semiconductors with excess of electrons) or type-p (semiconductors with an excess of positive charges, called holes), though in both cases the material is electronically neutral (Figure 2).

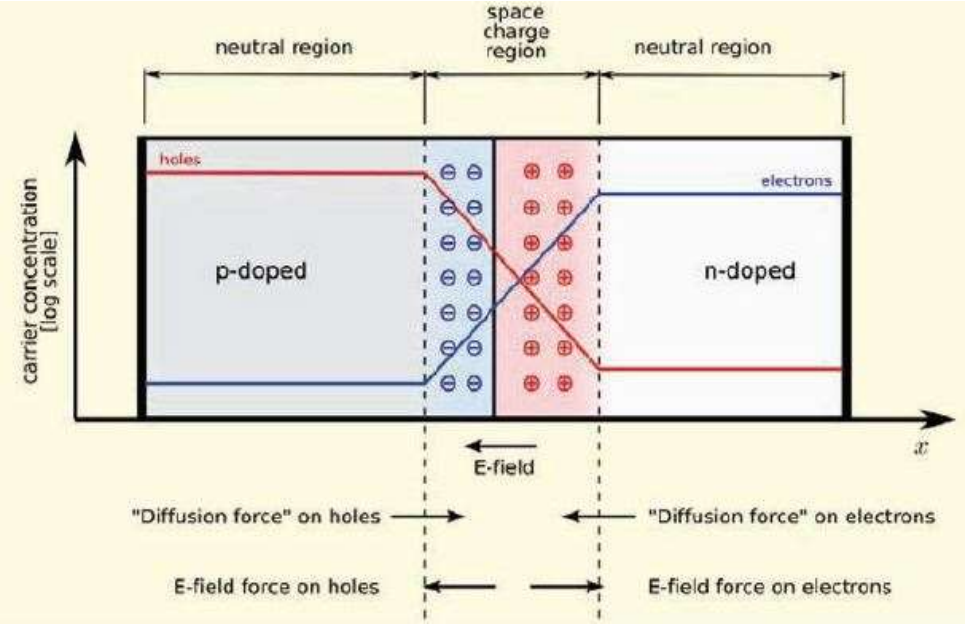

Figure 2: Schematic representation of a photovoltaics cell, showing the n-type and p-type layers.

As shown in Figure 2, the holes flow from the p-region and electrons flow from the n-region through the p-n junction via diffusion current upon contact. In addition to that, the fixed ions near the junction known as space charge region generate an electrical field in the opposite directions to the diffusion, which leads to a drift current. At equilibrium, the diffusion current is balanced with the drift current, so that the net current is zero.

When the PVC is in a relaxed state, the potential barrier is established at the p-n junction. As the light strikes the PVC, the energy contribution of the photons can be absorbed by the electrons, which can break their bonds, producing hole-electron pairs. These charge carriers are pushed by the electric field and conducted through the p-n junction. If an external load is connected, an electric current and a potential difference between the cell terminals will be established.

The different PVCs that have been developed to date can be classified into three main generations[6] and the aim of each generation is to reduce costs and improve efficiency compared to the previous one(s).

- First-Generation Photovoltaic Solar Cells:

The first-generation solar cells are based on single crystalline silicon (c-Si) or multi-crystalline silicon (multi-Si). Despite having good efficiency and stability, the indirect bandgap present in the crystalline silicon requires bulk of the material, which is cost-ineffective.

- Second-Generation Photovoltaic Solar Cells:

The second-generation solar cells are based on amorphous silicon, CIS/CIGS and CdTe due to their direct bandgap. The second-generation photovoltaic solar cells are more efficient in photons absorption, thus require thinner active layer as opposed to the bulk active layer in the first generation. The main issue with these materials is the instability upon prolonged period of exposure to the sunlight and their toxicity.

- Third-Generation Photovoltaic Solar Cells:

The third-generation solar cells can be thought as a more advanced version, where the aims are to realize highly efficient thin layer materials similarly to the second-generation solar cells[7], stable and non-toxic materials comparable to first-generation solar cells[8]. The main advantages of third generation PVCs are solution-processable technologies, suitable for large-scale production, mechanical robustness and high efficiencies at high temperatures. The most important technologies included in the third generation PVCs are: dye-sensitized solar cells (DSSCs); organic and polymeric solar cells (OSCs); perovskite cells and multi-junction cells. However, their key challenge is reducing the cost/watt of delivered solar electricity.

1.5. Organic solar cells

An organic solar cell is a type of photovoltaic that deal with conductive organic polymers or small organic molecules. The organic molecules are used for light absorption and charge transport to produce electricity from sunlight by the photovoltaic effect.

Interests in organic solar cells are caused by several factors such as the organic solar cells are lightweight, flexible, the organic molecules present in the organic solar cells are tunable, possess high optical absorption coefficients, the molecules are solution processable at high throughput cheaply and the organic solar cells have the potential to exhibit transparency (for application in windows) mean that it could potentially be the low-cost, innovative alternative for solar cells. In spite of that, organic solar cells suffer from efficiency. They offer about a third of the efficiency compared to inorganic solar cells and are prone to photochemical degradation[9], which implies low stability,[10] and less durable when compared to silicon based inorganic photovoltaic cells.

The prospects of low costs[11] and the potential in increased efficiency[12] for the organic solar cells favours them in the field of solar cell research. In fact, as of 2015, polymer solar cells were able to achieve over 10% efficiency via a tandem structure[13] and in 2018 was reached a record-breaking efficiency of 17.3%[14].

1.5.1. General principles of photovoltaic cells

When describing photovoltaic cells, band diagram is used to represent important energetic levels as a function of a spatial dimension. The following quantities are particularly important:

- Valence band (E_V) which is the highest occupied energy band (HOMO)
- Conductive band (E_C) is the lowest un-occupied energy band (LUMO)
- Energy gap ($E_{GAP} = E_C - E_V$) is the difference between the energy of the lowest unoccupied energy band and the highest occupied energy band

When the material absorbs sufficient photons, electrons in the valence band will be promoted into the conductive band in order to become a free negative charge. At the same time, this process would leave an empty state in the valence band, which would act as a free positive charge (hole). Therefore, the E_{GAP} is an important quantity that

defines whether a material is a conductor (E_{GAP} ≈ 0 eV), a semi-conductor (E_{GAP} ≈ 1 eV) or an insulator (E_{GAP} > 5 eV). The most vital part of solar cells are the semi-conductors, in which the energy required for an electron in the valence band to be promoted to the conductive band can be provided by solar energy. When an electron is in the conductive band, it is free to flow within the material, leaving an empty energy state in the valence band, and creating the electron-hole pair. Such a process can occur if the equation below is satisfied.

$$E_{PH} > E_{GAP}$$

Where the E_{PH} is the energy of the photon and it must be greater than the energy of the bandgap. Once the electron is promoted to the conduction band, the carriers can then either be moved by diffusion or driven by an electric field until they are collected at the electrodes. For instance, in silicon solar cell, a p-n junction provides the electrical field that helps drive the carriers towards the respective electrodes, hence generating a photocurrent. Organic solar cells on the other hand obey similar principles with slight difference in which the route of the excited electron travels.

1.5.2. Organic Solar Cells (OSC) working principle

Contrary to inorganic solar cells such as single crystalline silicon, in organic solar cells a photon is absorbed by an organic material which gives rise to an electron-hole pair called an *exciton*. An exciton needs some energy in order to be separated into a free electron and a hole pair. Such a separation can occur owing to effective fields. By tuning the blend of two materials (known as heterojunction) with suitable chemical potential difference, the effective fields present break the electron-hole bond.

The material which is donating an electron when separating the exciton is called a donor, and is characterized by a high LUMO (lowest unoccupied molecular orbital and equivalent to the conductive band), while the material which is receiving an electron when separating the exciton is called an acceptor, and is characterized by a low HOMO (highest occupied molecular orbital and equivalent to the valence band).

The basic working principle of an organic solar cell, schematically illustrated in Figure 3, is the following:

1. A photon with an energy $E_{PH} > E_{GAP}$ is absorbed by the active layer, forming an exciton.
2. The exciton can diffuse (on the order of the tens of nanometres before recombining) until it reaches a donor-acceptor interface.
3. The exciton can separate thanks to the potential at the donor-acceptor interface, forming two free carriers, one positive and one negative (also called polarons).
4. The charge carriers can diffuse across the materials driven by chemical potential toward the respective electrodes.

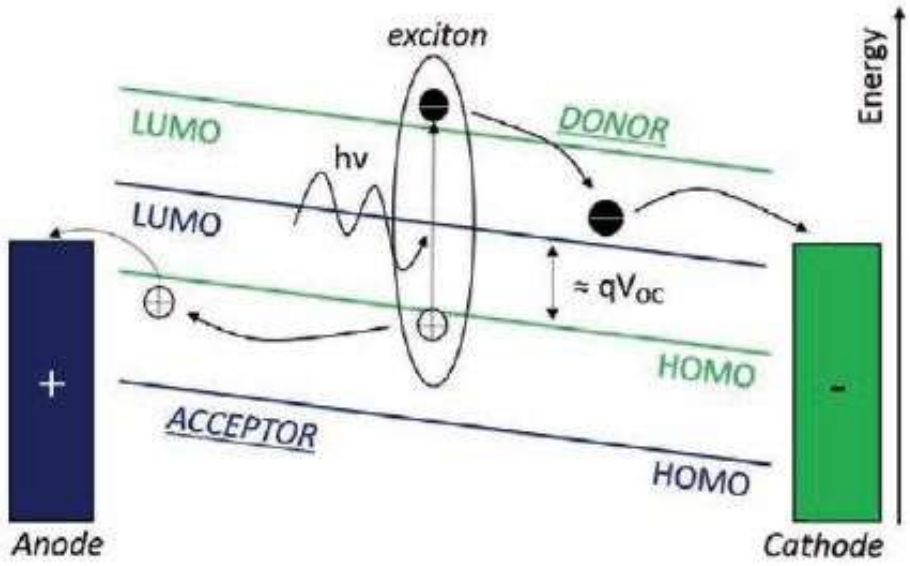

Figure 3: A photon with energy hν generates an exciton that separates into a positive and negative polaron. The charges are then collected at the electrodes

The number of electrons that are released by the exciton and collected at the electrodes when irradiated by photons is defined as solar cell quantum efficiency.

In particular, the ratio of the collected electrons divided by the number of incident photons, for a given energy, defines the External Quantum Efficiency (EQE):

$$\text{EQE} = \frac{electrons/sec}{photo \quad /sec}$$

While the ratio of the collected electrons divided by the number of photons absorbed by the active layer, for a given energy, defines the Internal Quantum Efficiency (IQE):

$$\text{IQE} = \frac{electrons/sec}{absorbed\ photons/sec}$$

More generically, the ratio of the output power divided by the input power is called Power Conversion Efficiency (PCE):

$$PCE = \frac{Pout}{Pin} = \frac{Vmpp \times Jmpp}{Pin} = FF \times \frac{Jsc \times Voc}{Pin}$$

Where P_{IN} is the power irradiating the solar cell, P_{OUT} is the maximum power at the output with V_{MPP} and J_{MPP} respectively the voltage and current at the Maximum Power Point (MPP). The parameters such as J_{SC}, V_{OC}, and FF are derived from the experimental current-density-voltage (J-V) curve as presented in Figure 4.

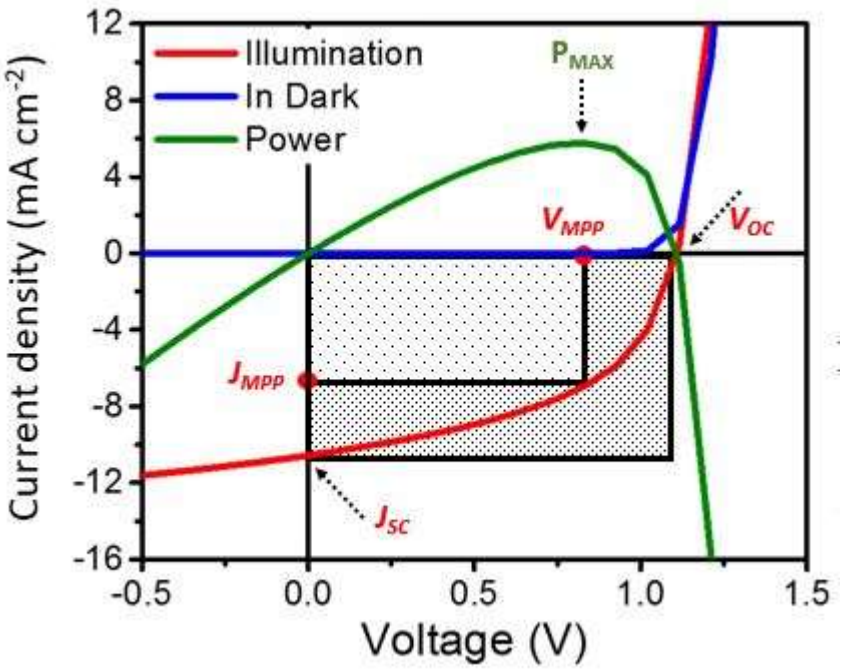

Figure 4: A schematic of a current-voltage graph for organic photovoltaic devices. Blue Curve: in dark; Red Curve: under illumination; V_{OC}: open-circuit voltage; J_{SC}: short-circuit current; V_{MPP}: voltage at max. power point; J_{MPP}: current at max. power point.

The fill factor (FF) is defined as the ratio between the MPP and the product of the open circuit voltage (V_{OC}) and short circuit current (J_{SC}). In organic photovoltaics, FF is essentially a measure of the quality of the cell compared to theoretical power that could

be generated. It is the quotient of the maximum power value and the product of the open circuit voltage and short circuit current:

$$FF = \frac{Pout}{Voc \times Jsc} =$$

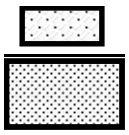

The short circuit current (J_{SC}) is the maximum photocurrent generation value[15]. It corresponds to the y-intercept value of standard current-voltage curve in which current is plotted along the y-axis and voltage is plotted along the x-axis, as seen in Figure 4. Within organic solar cells, the short circuit current can be impacted by a variety of material factors. These include the mobility of charge carriers, the optical absorption profile and general energetic driving forces that lead to a more efficient extraction of charge carriers.

The open circuit voltage (V_{OC}), is the difference of electrical potential between two electrodes when there is no external electrical current running through the device. This corresponds to the x-intercept on a current-voltage curve. Within bulk heterojunction organic photovoltaic devices, this value is highly dependent on HOMO and LUMO energy levels and work functions for the active layer materials.

The efficiency depends on the architecture of the active layer, which deeply affects the probability of separating an exciton. The most basic architecture is a bilayer device, which was used by Tang in 1986 in order to make the first demonstration of a working organic solar cell[16]. However, this structure suffered from low efficiency due to the short diffusion length of the exciton in an organic solar cell. Approximately ten years later, G. Yu et al. introduced the bulk heterojunction (BHJ) solar cell. In such a device, the interpenetrating mix of donor and acceptor provided large interfacial areas that increased the exciton dissociation rate by reducing the distance that the carriers needed to travel before dissociation[17].

A common quantity used to describe the irradiating light is the *irradiance*, measured in W/m^2, which must be multiplied by the active area of the device in order to obtain the input power P_{IN}. The OSC active area is the area where the top and bottom electrodes overlap. The efficiency depends on several material properties which affect for instance the V_{OC}. In fact, the open circuit voltage depends on the value of LUMO of the acceptor and on the value of HOMO of the donor:

$$qV_{OC} \approx E_{LUMO}(acceptor) - E_{HOMO}(donor)$$

where q = 1.6 x 10^{-19} C is the elementary charge, while E_{LUMO} (acceptor) and E_{HOMO} (donor) are the energy levels of the acceptor LUMO and of the donor HOMO respectively. Since V_{OC} is directly proportional to the PCE of the device, a lot of research groups have tried to synthesize donors with a low HOMO, in order to increase the value of the V_{OC}. However, lowering the HOMO also causes a larger E_{GAP} of the donor, since the position of the LUMO cannot be moved much in order to guarantee a good exciton separation[18]. A larger E_{GAP} implies less solar spectrum absorbed (since less photons can satisfy) and as a consequence less collected carriers and a lower efficiency. Therefore, in order to optimize the device efficiency, a compromise exists between V_{OC} and J_{SC}.

1.6. Junction types:

1.6.1. Single layer

Single layer organic photovoltaic cells are the simplest form. Where the organic molecule is placed between two electrodes. The top electrode shown in Figure 5 is typically Al, Mg or Ca and the bottom electrode is typically ITO-coated substrate such as glass.

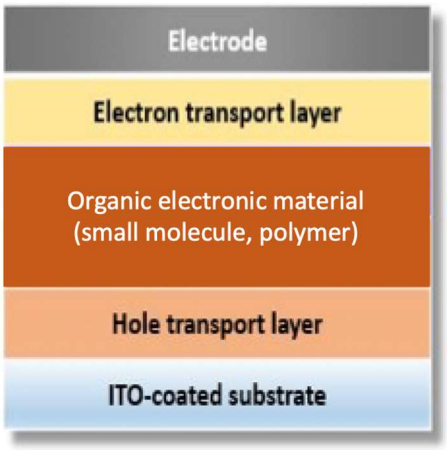

Figure 5: Sketch of a single layer organic photovoltaic cell

Upon shining light, the organic layer absorbs photon, as the ITO-coated glasses are transparent. As described previously, the organic layer will form excitons due to the excitation of electrons in the HOMO to the LUMO. The issue with single layer organic photovoltaic cells is that the effective electrical field is often too weak to free the

electron present in the exciton and frequently the electrons recombine with the holes without reaching the electrode[19,20].

1.6.2. Bilayer

Bilayer cells contain two layers, namely electron donor and electron acceptor in-between the conductive electrodes (Figure 6). The purpose of having a donor and acceptor layer was to minimise the issue mentioned in the single layer cells.

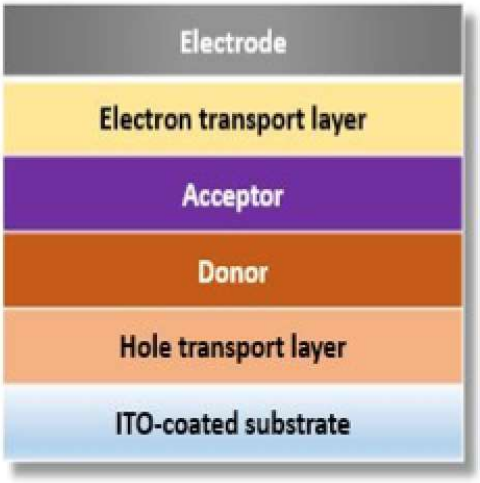

Figure 6: Sketch of a multilayer organic photovoltaic cell, Planar Heterojunction (PHJ)

This bilayer structure utilises the difference in electron affinity and ionisation energy between the donor and acceptor layer, more commonly known as a planar donor-acceptor heterojunction. The issue with this set-up was that the thickness of a polymeric layer to absorb enough light is at least 100 nm whilst the excitons have characteristic diffusion length of about 10 nm. This simply means that only minimal amount of excitons can reach the heterojunction interface before recombination of electrons with holes.

1.6.3. Bulk heterojunction

Bulk heterojunctions aim to utilise the same principle of the donor acceptor in bilayer at the same time minimizing the issue present in the bilayer cells. To do so, donor and acceptor materials are blend together as a bulk mixture as shown in Figure 7. This allows the short-lived excitons to reach the interface and dissociate to the acceptors without compromising the thickness of donor acceptor layer.[21] Though, efficient bulk heterojunctions need to maintain large enough domain sizes to form a percolating

network that allows the donor materials to reach the hole transporting electrode and the acceptor materials to reach the electron-transporting electrode. This percolating network is essential as it minimises the chances of the charges being trapped in donor or acceptor rich domain and undergo recombination.

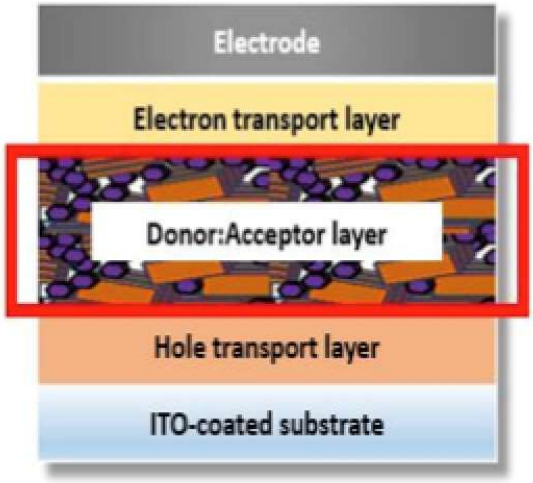

Figure 7: Sketch of a dispersed junction photovoltaic cell, Bulk Heterojunction (BHJ)

The bulk heterojunctions are typically composed of a conjugated molecule-based donor and fullerene-based acceptor.

The bulk heterojunction organic solar cells tackle the issue present in the planar cells as the distance between donors and acceptors are suited for carrier diffusion. This in turn allows the electron separated from the exciton and diffuse to the collecting electrode.

1.7. Recent directions for bulk heterojunction materials research

Recent progress in organic electronics had ignited great interest in the fundamental molecular design of the novel organic/polymeric semiconducting materials (SCMs) and in the optimal design of device architectures[22,23,24,25,26,27].

As mentioned before, the bulk heterojunction (BHJ) concept has been widely used for mainstream polymer solar cells (PSCs), in fact in BHJ-OSCs, the photoactive layer comprises electron-donor (D) and electron-acceptor (A) materials, blended in a BHJ structure. The donor materials can be the polymer or small molecule and the acceptors can be the fullerene derivatives or n-type organic molecules.

One approach to design highly efficient photovoltaic polymers is to couple at least an electron donor with an electron acceptor, either directly or through a conjugated bridge[28,29,30,31]. Consequently, these polymers form a more favourable energy level for electron as shown in Figure 8. By using a "weak donor" material, a low HOMO energy level can be achieved due to the narrow bandgap (Eg < 1.6 eV). In contrast, a "strong acceptor" material possesses spectral coverage that is complementary to that of the donor (1.6 < Eg < 2.2 eV) which in turn narrow the bandgap.

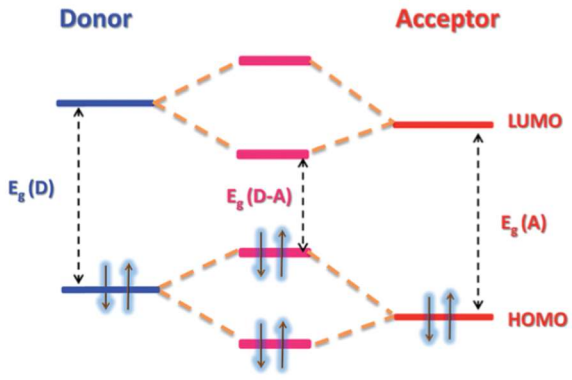

Figure 8: Hybridization of the energy levels of the donor and acceptor units lowering the bandgap of conjugated polymers.

The ideal conjugated polymer for BHJ solar cells should have a low lying HOMO energy level to ensure a high open circuit voltage (Voc), a broad absorption in the range of 300–900 nm to maximize the short-circuit current density (Jsc) and a high charge mobility to improve the fill factor (FF).

Both the p-type (hole-transporting) and n-type (electron-transporting) organic/polymeric semiconductors, presented in Figure 9, are expected to play a role in tomorrow's electronics.

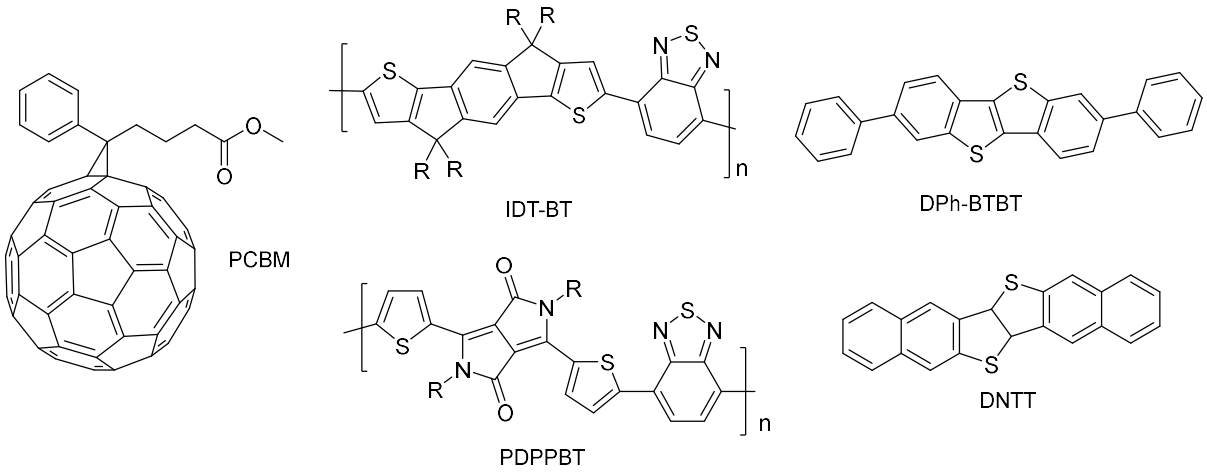

Figure 9: Principal organic conjugated semiconductors.

1.8. Non-fullerene acceptor for organic solar cells

The fullerene acceptors have been the standard for most organic photovoltaics in the last years but due to their weak properties (instability, poor optical absorption and their limitation in energy tunability), the non-fullerene organic solar cells (NF-OSCs) have been paid increasing attention. Traditional OSCs utilize fullerene acceptors, typically [6,6]-phenyl-C_{61} (or C_{71})-butyric acid methyl ester ($PC_{61}BM$[32] or $PC_{71}BM$) as the electron- acceptor materials (see Figure 10), while n-type organic molecules are selected to replace fullerene as the acceptor materials in NF-OSCs.

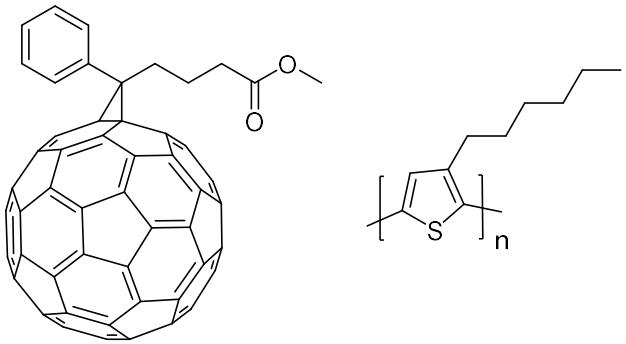

Figure 10: $PC_{61}BM$ it is an electron acceptor material (left) and it is often used in organic solar cells or flexible electronics in conjunction with electron donor material (right) such as Poly(3-hexylthiophene (P3HT).

Contrary to the fullerene acceptors, the chemical structure of the non-fullerene organic acceptors is more tunable through the chemical modification of the π-system. Therefore, it is possible to obtain a complete coverage of the solar spectrum credits to a design specific of the acceptor molecules combined with the donor.

1.9. Indacenodithiophene (IDT)

Amongst the various types of conjugated donor molecules, indacenodithiophene (IDT) has been recognized as a promising building block to construct narrow bandgap semiconductors for high-efficiency photovoltaics.[33,34,35] This is due to its coplanar fused ring aromatic structure and credits to strong intermolecular interactions can afford ordered molecular organization.

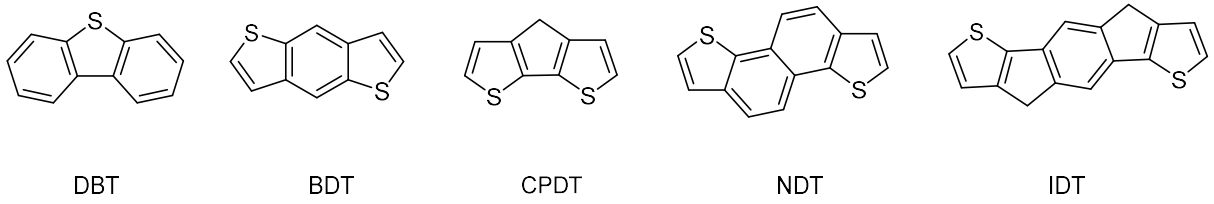

Figure 11: Building blocks: Dibenzothiophene (DBT), Benzodithiophene (BDT), Cyclopentadithiophene (CPDT), Naphthodithiophene (NDT) and Indacenodithiophene (IDT).

As shown in Figure 11, in contrast to the other building blocks such as Dibenzothiophene (DBT), Benzodithiophene (BDT), Cyclopentadithiophene (CPDT), Naphthodithiophene (NDT), the pentacyclic IDT molecule with a much-extended π-conjugated system could produce highly desirable photo-physical and electronic properties *i.e.* a low degree of energetic disorder and high carrier mobility. IDT unit has three aromatic rings integrated into a single fused molecular structure in which a bridging atom fixes coplanarity between the rings, maximizing the π orbital overlap, as well as reducing conformational energetic disorder.

Recently, Iain McCulloch and co-workers have developed an IDT-based polymer with a high hole mobility despite lack of long-range crystalline order[36]. This is mainly due to the remarkable resilience of the backbone conformation to side chain disorder[37].

Another feature of the IDT unit is that both the choice of bridging atom and the planarity of the substituents projecting from the bridge and/or through electron donation or inductive effects strongly influence the frontier molecular orbital energy levels and

distribution. The former influences the degree of aromaticity of the repeating units, while the latter has an effect on the electron density of the structural unit.

In addition, the bridging position also offers an opportunity to covalently graft different side chain groups; typically, alkyl chains or aromatic side chains, which can improve solubility and impact polymer thin film morphology, depending on their length and shape (Figure 12).

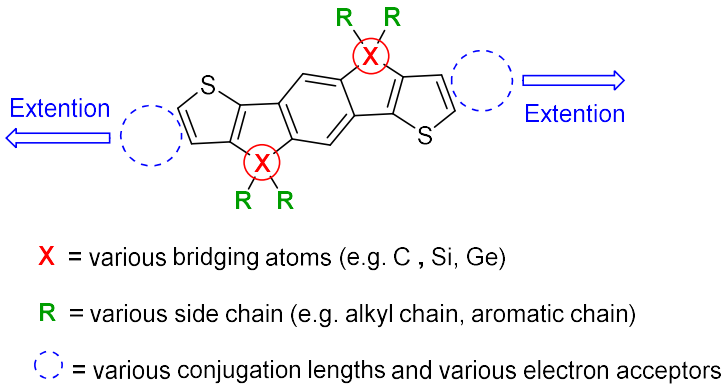

Figure 12: Design consideration of IDT units

Since the first introduction of an IDT unit into photovoltaic materials, hundreds of new IDT-based polymers have been synthesized through Stille coupling and/or Suzuki coupling reactions, suggesting that these materials have currently become one of the major families of polymer photovoltaic materials[38,39,40]. Recently, various IDT-derivatives based on non-fullerene electron acceptors have also been developed for photovoltaic applications[41].

1.9.1. IDT polymer based on electron acceptor 2,1,3-benzothiadiazole (BT)

The ability to absorb light from the near UV up to 700 nm is another major merit of the IDT-based copolymers for photovoltaic applications. The absorption profile can be easily tuned by varying the electron-deficient counterpart, and consequently strong absorption can be achieved in the low-energy region of the visible spectrum.

As one of the most promising acceptors suitable for construction of highly efficient photovoltaic materials, 2,1,3-benzothiadiazole (BT) with a relatively high electron affinity has a quasi-quinoidal structure rather than a heteroaromatic system. Its high electron affinity is the result of the imine functionalities with relatively low energy p*-orbitals. This molecule possesses a relatively low-lying HOMO energy level in the

resulting polymers, which is very favourable to achieve a high Voc[42]. Ting et al. were the first to synthesize an IDT and BT-based conjugated amorphous polymer (Figure 13)[43], with a high PCE of 6.4%, a larger Jsc of 11.2 mA cm^{-2}, a Voc of 0.85 V and a quite high FF of 0.67. Following their report, several state-of-the-art IDT-based conjugated polymers were successfully developed soon after.

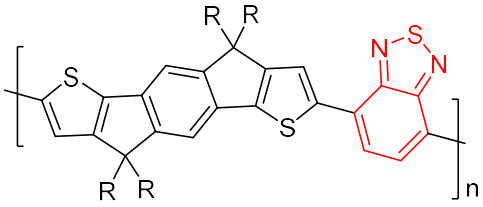

IDT-BT

Figure 13: Chemical structures of IDT-based polymer with benzothiadiazole (BT) derivative as acceptor

1.9.2. IDT polymers based on various side chains

By spin coating or blade-coating a polymer solution (if materials are highly soluble in organic solvents), one can easily fabricate large-area thin film photovoltaic devices. In particular, for solution-processable PSCs the solubility of the polymer is one of the key factors affecting film morphology and device performance. As reported in many literature studies, the introduction of side chains onto the polymer backbone is the most effective way to tune and improve the polymer solubility since the side chains can induce the backbone twisting as well as increase the interchain distance. For that reason, the size and shape of the side chains play an important role in molecular orientation and π-π stacking of the polymers and influence the charge transport and the miscibility of the acceptors. IDT-based polymers could be divided into two parts: one-part concerns substitution of the IDT units by aromatic side chains; the other deals with the grafting of alkyl side chains on the IDT units. Studies show that replacement of the aromatic side chains with the alkyl side chains with less steric hindrance would make the polymer backbone to aggregate easily[44], which will be beneficial for charge transport (Figure 14). This means that by choosing appropriate side chains, it is possible to control the optoelectronic properties of polymers.

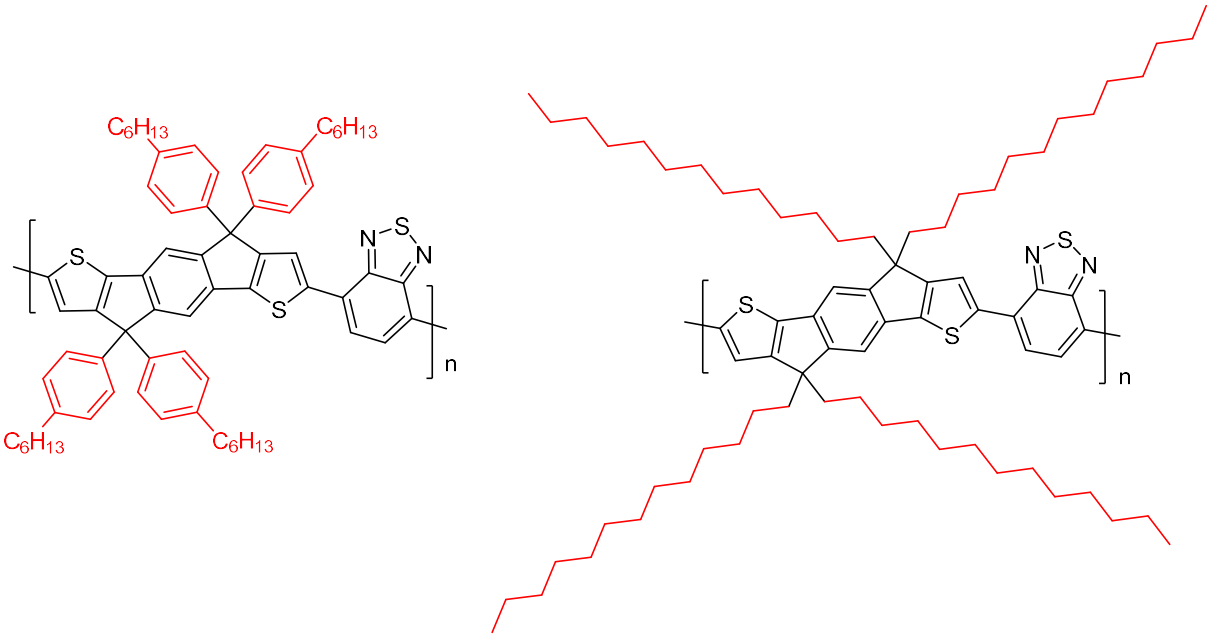

Figure 14: Chemical structure of IDT-based polymers with various side chains (aromatic and alkyl)

1.9.3. IDT polymers based on various bridging atoms

Most of the high-performance polymers for state-of-the-art BHJ solar cells mainly rely on thiophene or thiophene-based heterocycles. The heteroatoms can induce a variety of intermolecular interactions that are essential for achieving excellent device performance by affecting the electron density and molecular planarity. A series of soluble IDT-BT based D–A copolymers were designed and synthesized, where a single bridging atom in the IDT unit varied from C to Si to Ge (Figure 15)[45,46,47].

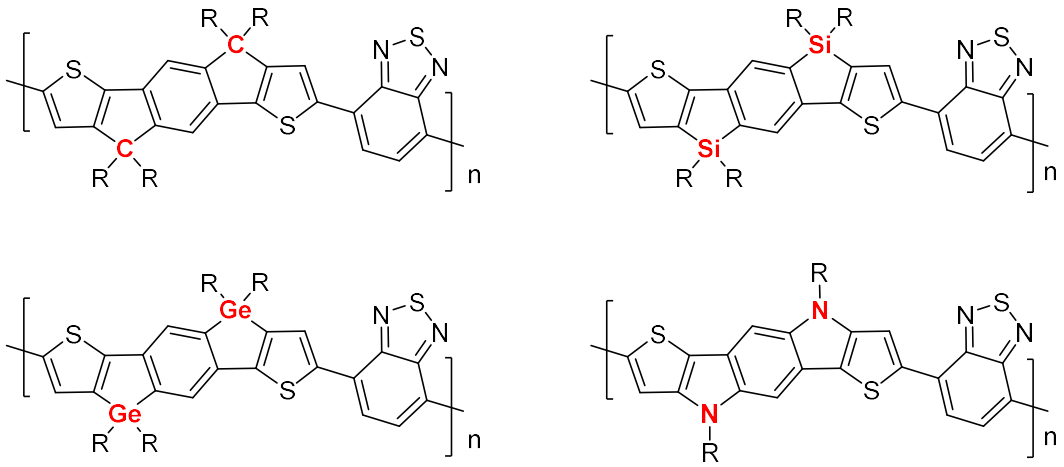

Figure 15: Chemical structure of IDT-based polymers with various bridging atoms

As a result, heavy atom substitution leads to the polymer being crystalline. Unlike the amorphous polymer with C, both Si and Ge show clear indications of semi-crystalline behaviour due to the longer C–Si or C–Ge bond relative to the C–C bond, which reduce the steric hindrance from the bulky alkyl side chains.

This result indicated that bridging atom variation in the IDT unit could be used to control the molecular packing behaviour of the polymers but has a little effect on the optical bandgaps. Moreover, a strong correlation between the polymer molecular weight and the absorption and photovoltaic performance has demonstrated that the high molecular weight polymer could provide the best performance in those categories.

In addition to the above-mentioned three elements (C, Si, Ge) as the bridging atoms of the IDT unit, the more electron donating nitrogen atom (N) can also be the bridging heteroatom of the IDT unit. Incorporation of a strong electron-donating atom would further promote molecular orbital hybridization leading to a reduction in the bandgap of the polymer and enhance the electron density of the ring. Additionally, the electron-rich nature of the polymer backbone would be favourable for hole transport.

1.9.4. IDT polymers based on various conjugation lengths

The highly fused aromatic/heteroaromatic units, in which the covalently rigidified adjacent units could prevent rotational disorder to reduce reorganization energy, which lead to improved charge carrier mobilities, enhance effective conjugation of the polymer backbone to facilitate electron delocalization.[48,49]

In order to enhance the charge mobility and device performance of the fused-ring polymers, the IDT unit can be further extended by incorporating two thieno[3,2-b]thiophene (TT) units. The extended IDT system with two outward TT units replacing the thiophene moieties on IDT was designed to form a novel seven-ring indacenodithieno[3,2-b]thiophene (IDTT) donor unit as shown in Figure 16.

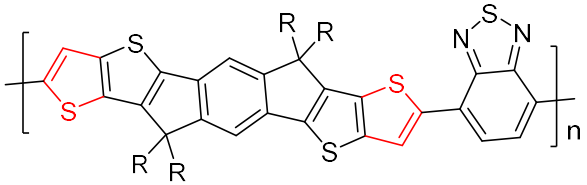

Figure 16: Chemical structure of IDT-based polymer with enhanced conjugation length.

The extension of the effective conjugation length and planarity improve chain packing. This is also an effective way to reduce the bandgap and improve charge transport for high-efficiency photovoltaic devices. As mentioned previously, the variation of the bridging atom of the IDT unit could be used to control the molecular packing properties but has a little effect on the optical bandgap of the resultant polymer.

1.10. Design and synthesis of the IDT based non-fullerene acceptors

With the fast development of new organic semiconductor materials and the great improvements in the optimization of device architectures, organic photovoltaics based on composites of a conjugated polymer as the electron donor and a fullerene/fullerene derivative as the acceptor have seen a rapid progress in PCE over the past few years.

In comparison with the polymer donor materials utilized for BHJ devices, the development of electron acceptor materials lags far behind the rate of innovation of PSCs. To date, electron acceptors used in the vast majority of PSCs are fullerene and its soluble derivatives (e.g., $PC_{61}BM$, $PC_{71}BM$ and others). These fullerene-based electron acceptors can offer several attractive advantages in the polymer: acceptor blends-based BHJ devices:

- three-dimensional electron transport;
- multiple reversible electrochemical reductions;
- high electron mobilities;
- formation of both pure and mixed domains of the appropriate length scale for charge separation.

However, the disadvantages of these acceptors include high cost of purification and production, poor overall yield, relatively narrow spectral range of optical absorption compared to the solar spectrum, limited energy level variability due to synthetic inflexibility, device instability resulting from an inherent tendency to undergo post-fabrication crystallization and more have also been found in the practical PSCs.

The greatest challenges in developing more efficient non-fullerene acceptors are the narrow absorption spectrum, the absence of semiconductors that can integrate solution processability with suitable electron-transport properties and energy levels. Among all the non-fullerene acceptors reported in the past several years, the promising

IDT-based acceptor materials for high performance BHJ PSCs have attracted much attention due to their rigidified coplanar structures, which can efficiently restrain rotational disorder and consequently lower reorganization energy, 3D conformation that is very critical to non-fullerene materials, the tunability of molecular and electronic properties by chemical modification. Most of the high-performance non-fullerene acceptors reported so far mainly rely on A-D-A structures. The LUMO levels of acceptors are mainly determined by the A groups and if the electronegativity of the A group can be reduced, it will be possible to obtain non-fullerene acceptors with an elevated LUMO level and hence improved Voc in PSCs.

1.11. State of the art

In a previous work published from my research group at KAUST, a new series of non-fullerene acceptors based on fluorene core called FBR has been specifically designed to give improved performance alongside the wide band gap donor poly(3-hexylthiophene). A polymer with good prospect for commercial OPV due to its relative scalability, stability and to the high efficiency was obtained. It owned the highest efficiency for a fullerene-free device when it was first reported[50]. (Figure 17).

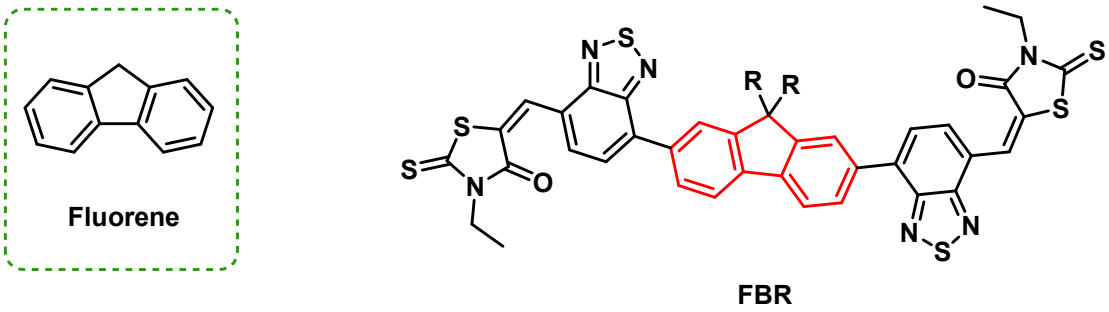

Figure 17: Fluorene unit and related non-fullerene acceptor (FBR) based on fluorene core

However, the short-circuit current (Jsc) in these devices was limited and the large extent of spectral overlap of FBR with P3HT and lack of long-wavelength absorption reduced the ability to harvest photons across the spectrum, further limiting the generated photocurrent. Hence the need to realize better acceptor derivatives in order to push forward this technology.

2. Aim

This thesis is a comprehensive report of my internship at the King Abdullah University of Science and Technology (KAUST), in KAUST Solar Centre (KSC), Saudi Arabia.

In order to find new non-fullerene acceptors for OPV applications, new functionalizations of the indacenodithiophene (IDT) donor were investigated during my thesis project. In particular, it has been considered the possibility of adding benzothiophene (TB) units next to the thiophene moieties and side chains (R) within the IDT. (Figure 18).

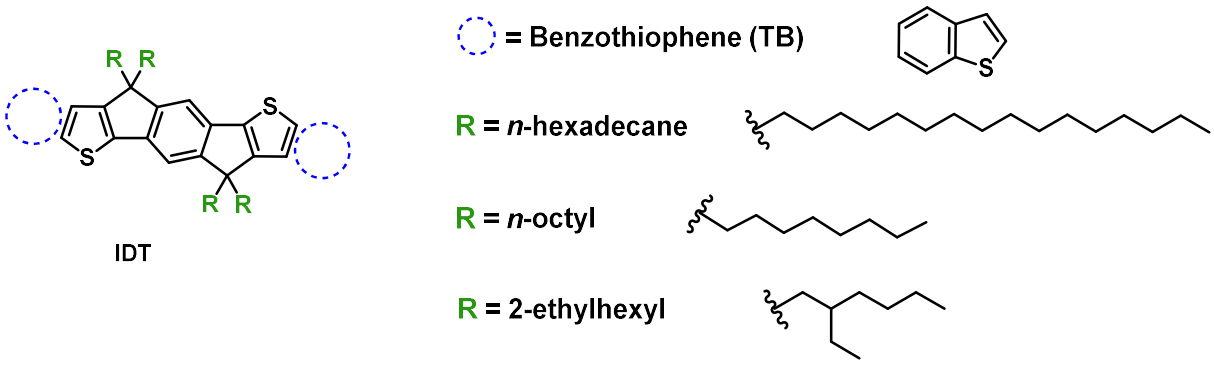

Figure 18: IDT core with benzothiophene (blue circle) and R side chains

The purpose of adding benzothiophene (TB) is to extend the conjugation length in the fused-ring in order to increase the HOMO energy level, thus narrowing the band gap which results in a significant red-shift in the absorption spectrum. By adding different side chains (R) in the IDT, we may increase the polymer solubility that is one of the key factors affecting the film morphology and device performance of the organic solar cells.

3. Results and discussion

This section of the thesis will be divided into three sub-headings. Section 3.1 will comprise the synthesis of the indacenodithiophene (IDT) unit. Section 3.2 will comprise the synthesis of the TBIDT-BT polymer. This is followed by section 3.3, which includes design synthesis of other new non-fullerene small molecule acceptors based on IDT unit, alkylated with linear (n-octyl)- or branched (2-ethylhexyl)- side chains, indicated as O-TBIDTBR and EH-TBIDTIR, respectively. Lastly, in section 3.4 the synthesis of the novel deuterated compound IDT-BR for future morphology studies will be reported.

3.1. Synthesis of indacenodithiophene (IDT)

The indacenodithiophene (IDT) core was synthesized according to the literature procedures[51,52] and the synthetic route is shown in Scheme 1.

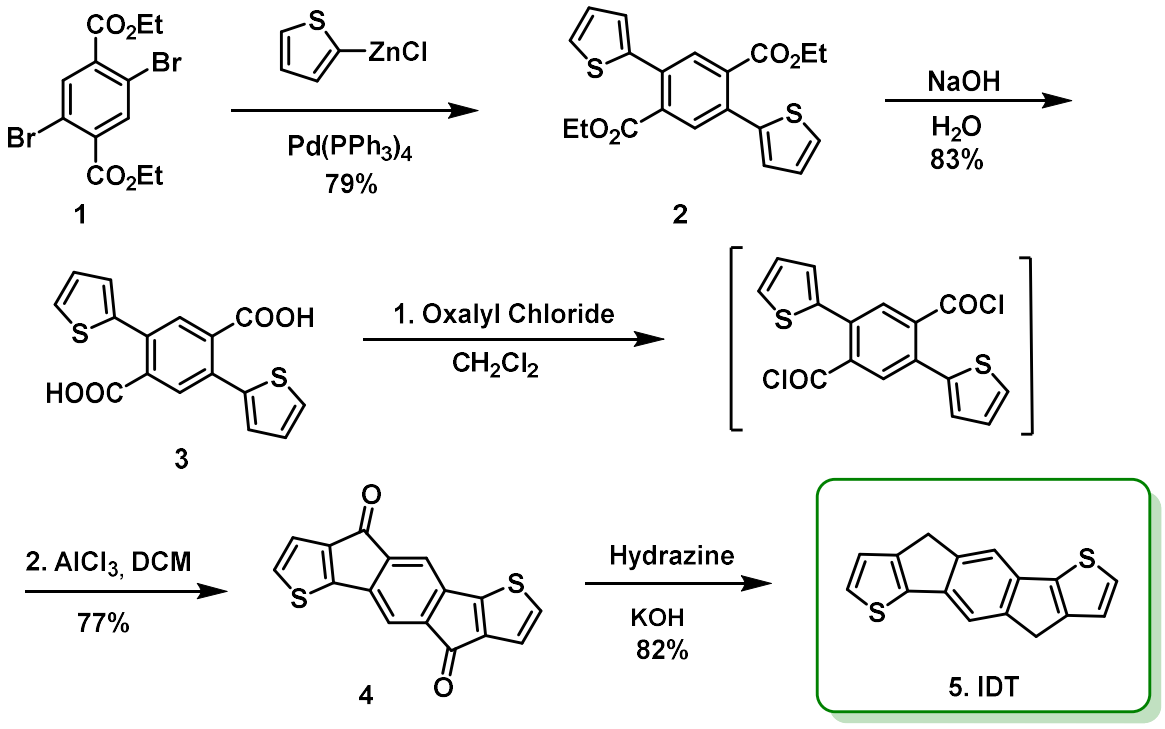

Scheme 1: Synthetic route to IDT unit

The first step is a Pd-catalyzed Negishi coupling reaction between the diethyl 2,5-dibromoterephthalate and the 2-thienylzinc chloride that gave compound **2,** derived form the double cross-coupling, in 79% yield. Subsequently, the compound **2** was saponified in the presence of aqueous NaOH to give the dicarboxylic acid **3**. The

compound **3** was treated with oxalyl chloride in DCM to obtain the acyl-chloride intermediate which, in turn, was subjected to intramolecular Friedel-Crafts reaction to give the diketone **4** in good yield (77%). The last step was a Wolff-Kishner reduction to convert the dicarbonyl groups into methylene groups thus forming the IDT core with good yield.

The IDT was used as starting material for the syntheses described below.

3.2. Synthesis of the novel TBIDT-BT polymer

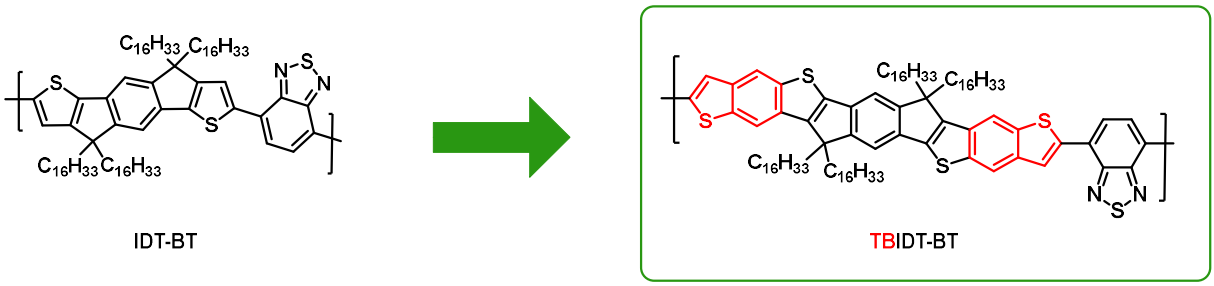

Figure 19: Structure of IDT-BT, and of the novel TBIDT-BT acceptor

The synthesis of TBIDT-BT started from the idea to modify IDT-BT[52], an already known material for photovoltaic devices indicated in Figure 19 (left). The modification was designed by inserting a benzothiophene (TB) unit, as shown in TBIDT-BT (red in Figure 19). The purpose of adding the TB unit is to narrow the band gap, thus planarizing the molecular structure and significantly red-shifting the absorption by increasing the HOMO energy level. Besides that, TBIDT-BT should crystallize better than IDT-BT due to its unique morphology. Moreover, the development of this kind of compounds would result in better prospects for commercial OPV, due to their scalability and stability.

The synthetic route to obtain the novel non-fullerene polymer acceptor TBIDT-BT starting from IDT material is depicted in Scheme 2.

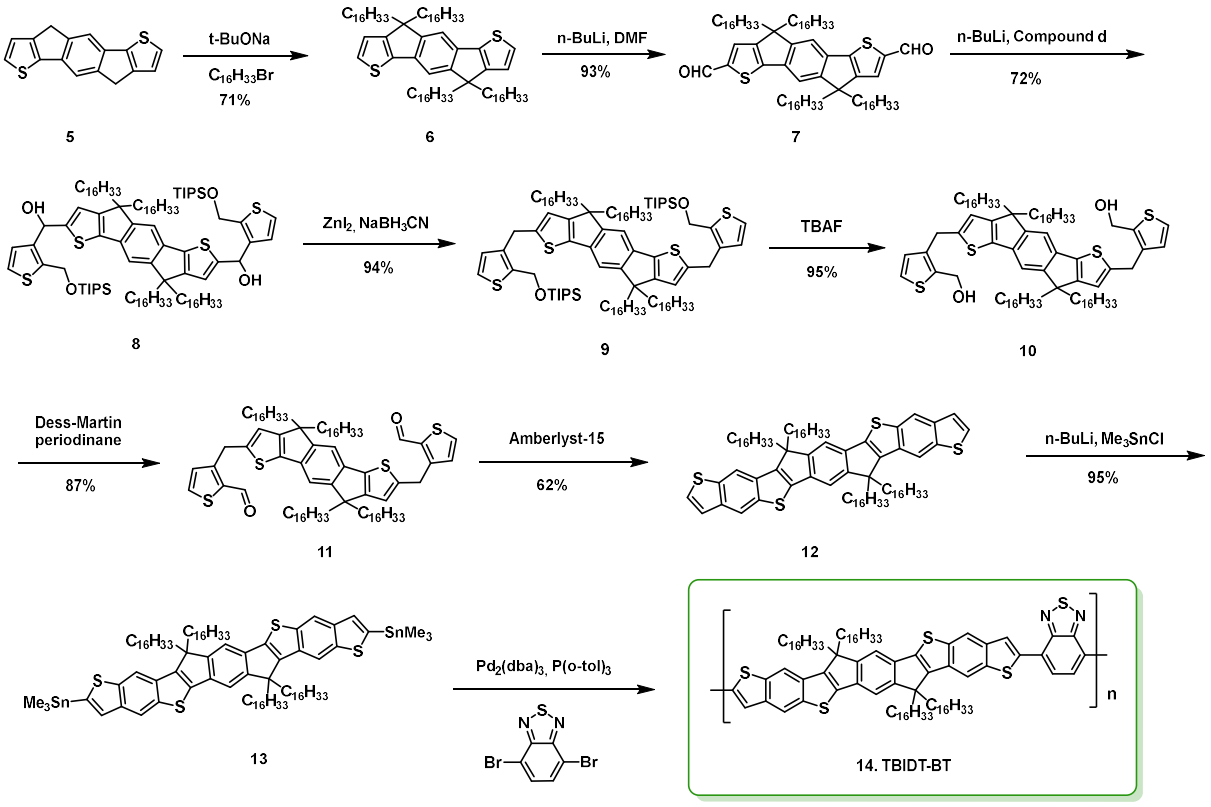

Scheme 2: Synthesis of TBIDT-BT polymer from IDT

The compound **5** (IDT) was subjected to basic treatment with sodium tert-butoxide to give a carbanion that was, *in situ*, treated with 1-bromohexadecane. After chromatographic purification on silica gel the tetraalkylated compound **6** was isolated in 71% yield. Subsequently, compound **6** was treated with *n*-butyllithium solution (in *n*-hexane) and *N*,*N*-dimethylformamide (DMF) with formation of an aldehydic group in alpha position to each thiophene sulphur atom, thus producing compound **7**. It was then treated with *n*-butyllithium and compound **d** (prepared separately, synthesis shown in Scheme 3) to provide compound **8** with a good yield (72%). Reduction of the hydroxy groups in **8** by treatment with zinc iodide and sodium cyanoborohydride gave rise to compound **9** that was then deprotected with tetrabutylammonium fluoride (TBAF) leading to compound **10** in quantitative yield. The latter was then oxidized to dialdehyde using the Dess Martin periodinane reagent and the dialdehyde **11** was reacted with Amberlyst 15, to give the cyclic compound **12**. The compound **12** was

then di-stannylated in the alpha position to thiophene rings by treatment with *n*-butyllithium followed by addition of trimethyltin chloride. Lastly, the TBIDT-BT was obtained through a Suzuki cross-coupling condensation between the di-stannyl derivative **13** and benzothiadiazole catalyzed by tris(dibenzylideneacetone) dipalladium(0) [$(Pd_2(dba)_3$] and tri(*o*-tolyl)phosphine [P(*o*-tol)$_3$].

The polymer TBIDT-BT thus obtained will be characterized and analysed later by my laboratory group. This synthetic route provides a well-defined backbone and, combined with the presence of linear alkyl side chains, optimisation is expected for the molecular packing.

The preparation of the compound **d** used in the above described synthesis of TBIDT-BT is shown in Scheme 3.

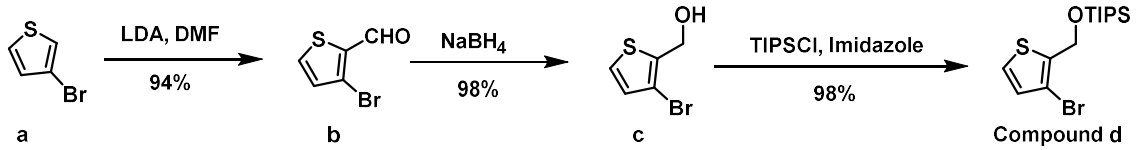

Scheme 3: Synthesis of compound **d**

The first step is an α-metallation with LDA of the thiophene **a** followed by DMF attack to obtain the aldehyde **b**. This product was treated with sodium borohydride ($NaBH_4$) to give the alcohol **c**. The last step was the protection of the hydroxyl group with triisopropylsilyl chloride (TIPSCl) to obtain the compound **d** that was used for the synthesis of TBIDT-BT, O-TBIDTBR and EH-TBIDTBR (see below).

3.3. Synthesis of the non-fullerene IDT-based small molecules O-TBIDTBR and EH-TBIDTBR as novel acceptors

The optimization of the different steps of the synthetic procedure to produce TBIDT-BT suggested to attempt the synthesis of novel IDT-based small molecules. The synthesis of a small IDT-based molecule is justified by the fact that small-molecule-based solar cells are generally less challenging, giving less variation of the product between every batch of synthesis when compared to polymer solar cells. Moreover, it is easier to tune their energy level and they are more stable.

With these considerations in mind, we planned to prepare novel small molecules, by inserting TB into IDTBR structures, already prepared in my research group. Thus, analogously to the concept described in section 3.2, we would be able to achieve similar improvement in terms of broader absorption spectra and better crystallization with the advantage of small molecule solar cells such as tunability and stability.

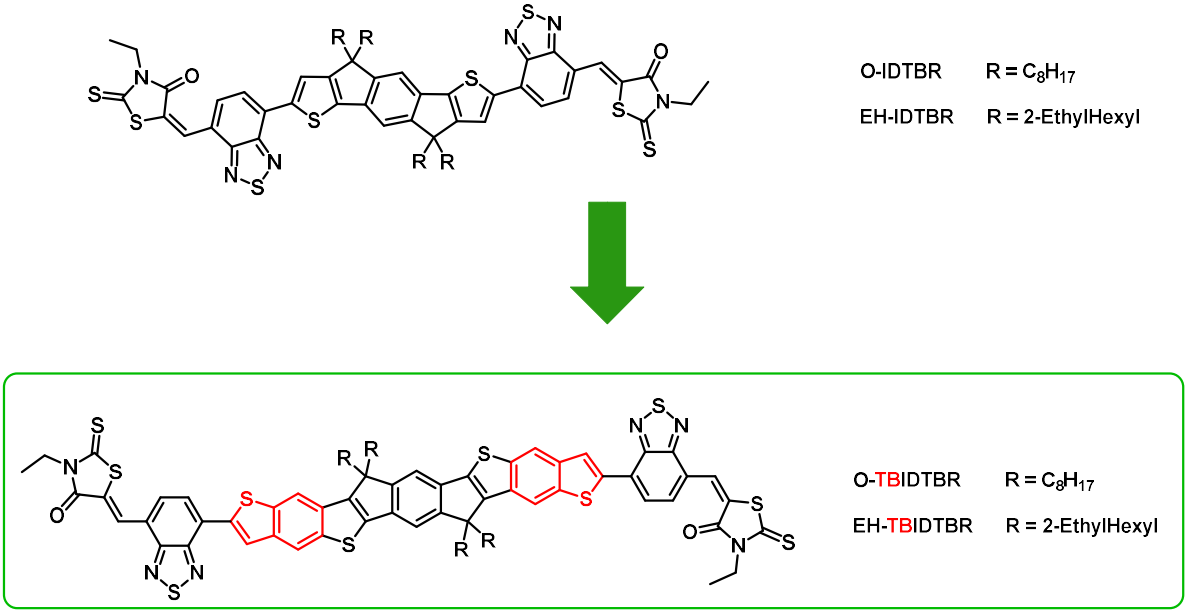

Figure 20 : Structure of O-IDTBR and EH-IDTBR, followed by the new O-TBIDTBR and EH-TBIDTBR acceptors

The synthetic routes to new non-fullerene small molecule acceptors O-TBIDTBR and EH-TBIDTBR are reported in Scheme 4. The first syntheses are similar to those shown in Scheme 2, with the difference that, in current cases, the alkylating agents were *n*-octyl- or 2-ethylhexyl- bromide. To obtain a small molecule, the di-stannyl derivative analogous to **13** in Scheme 2, was designed to react, through Suzuki coupling, with 7-

bromobenzo[c][1,2,5]thiadiazole-4-carbaldehyde to give TB-IDTBT. This dialdehyde, reacting with a rhodanine derivative, will produce the final product.

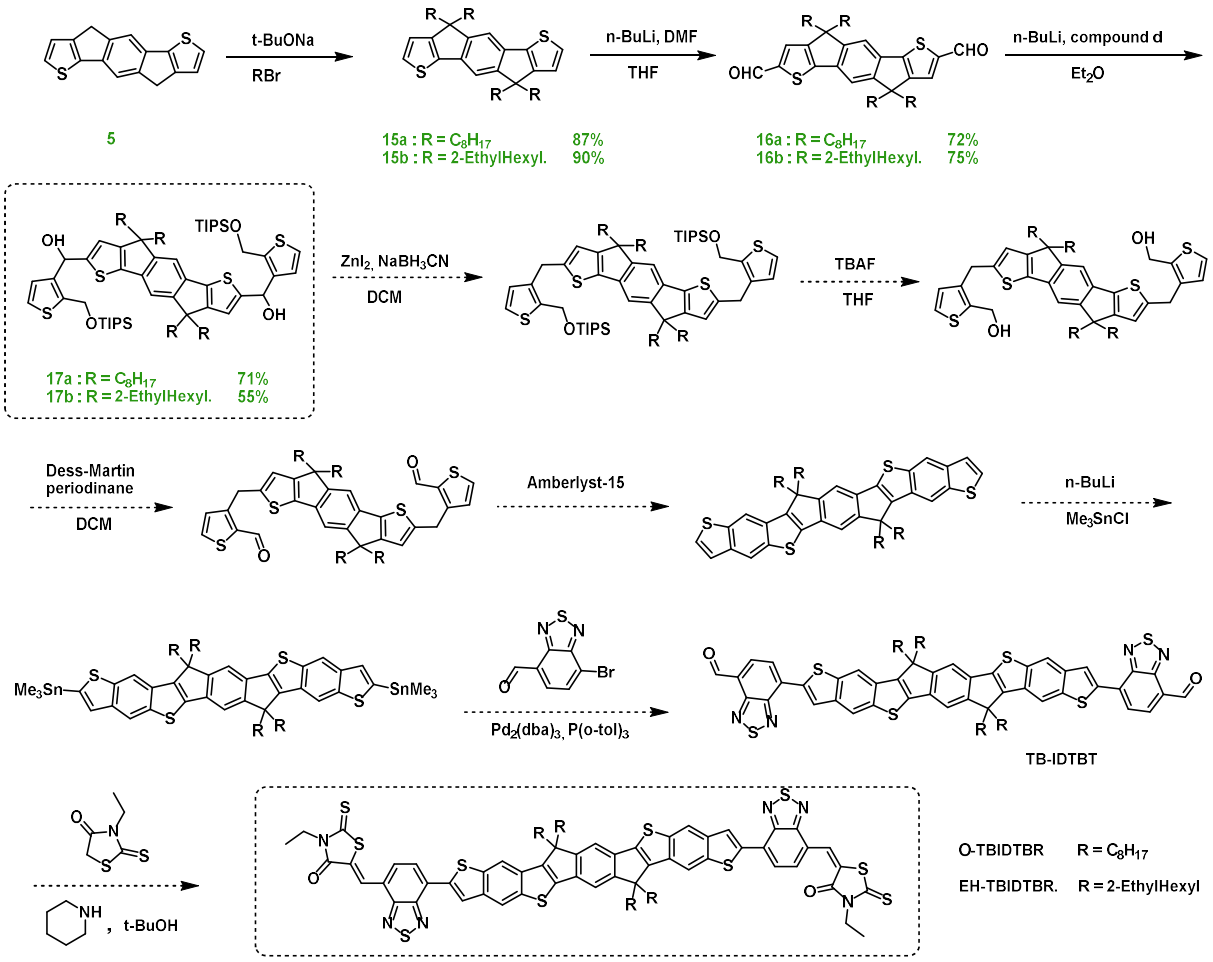

Scheme 4: Synthetic route of O-TBIDTBR and EH-TBIDTBR

In particular, compound **5** (IDT) was subjected to base treatment with sodium tert-butoxide followed by addition with an alkyl halide, namely 1-bromooctane or 2-ethylhexyl bromide and, after chromatographic purification on silica gel, the desired tetraalkylated products **15a** and **15b** were obtained in 87% and 90% yield, respectively.

Subsequently, the compounds **15a** or **15b** were deprotonated with *n*-butyllithium followed by reaction with *N*,N-dimethylformamide (DMF) introducing an aldehyde group in alpha position to each thiophene moiety, generating compounds **16a** and **16b** which, in turn, were treated with *n*-butyllithium and compound **d** (previously prepared, synthesis showed in Scheme 3) to provide compounds **17a** and **17b** with a good yield.

Because of the limited time of my internship, in which I also synthesized other compounds not described in this thesis due to not-disclosure agreements, the syntheses of Scheme 4 were not completed. The future plan will be the reduction of compound **17** to remove the hydroxyl groups followed by the addition of TBAF in order to remove the protecting group and form the dialcohol. After that, a mild oxidation will be carried out by the Dess-Martin periodinane in order to convert the alcohol into aldehyde (without further oxidation to carboxylic acid). Subsequently, the Amberlyst 15 (an acid catalyst that works as an ion exchange resin) will be used to perform a cyclization. The compound thus formed will be first stannylated with trimethyltin chloride, then reacted via Pd-catalyzed Stille coupling with the bromobenzo[c][1,2,5]thiadiazole-4-carbaldehyde followed by a Knoevenagel condensation with 3-ethylrhodanine to yield the final product.

3.4. Synthesis of a novel deuterated IDT-BR for future morphology studies

In an effort to understand the morphology of a small molecule (IDT-BR) discovered in the group previously to mine entrance in internship, we decided to replace the 3-ethylrhodanine groups present within the structure with deuterated 3-ethyl-d_5-rhodanine groups (Figure 21).

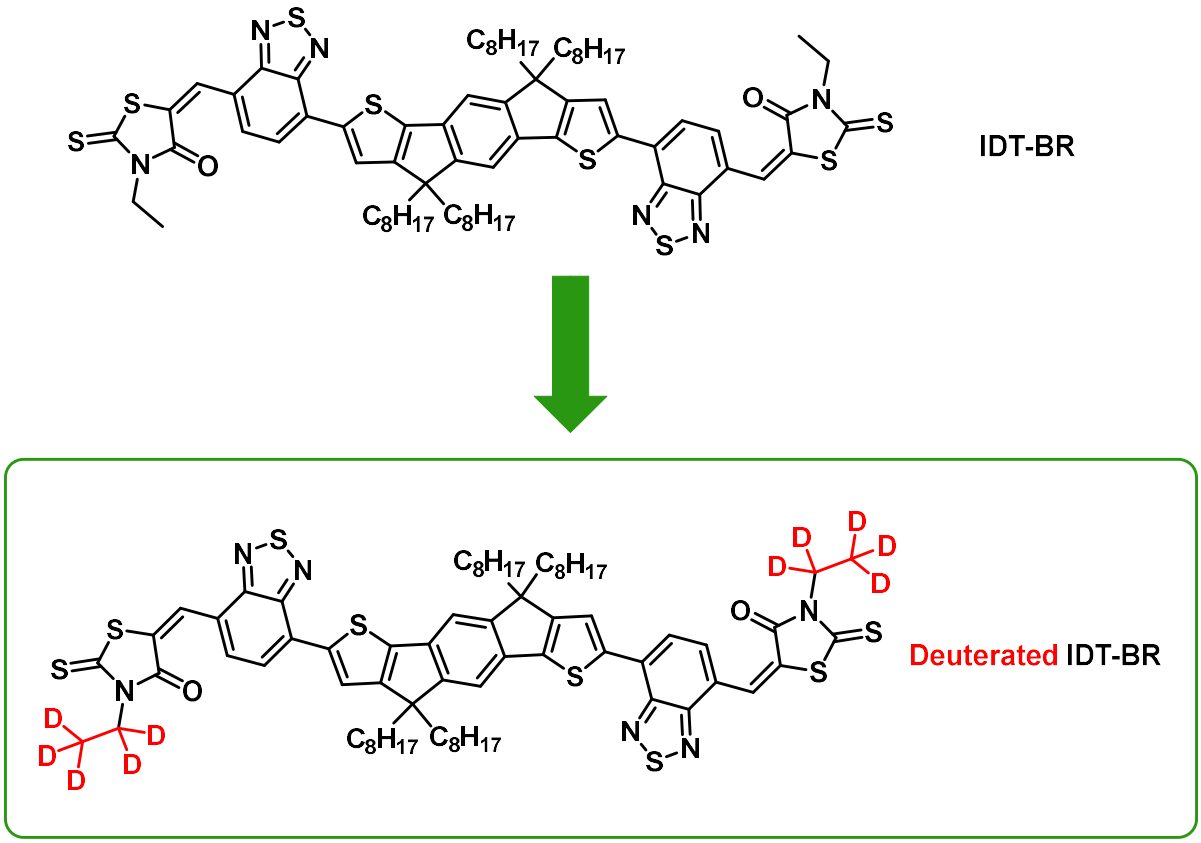

Figure 21: Structure of IDT-BR, followed by the novel deuterated IDT-BR

To made the deuterated compound **IDT-BR** it was necessary to previously synthesize two intermediates to be used during the synthetic pathway, namely 3-ethyl-d_5-rhodanine and 7-bromobenzo[c][1,2,5]thiadiazole-4-carbaldehyde (**I**).

The synthetic route to deuterated 3-ethyl-d_5-rhodanine (**g**) is showed in Scheme 5.

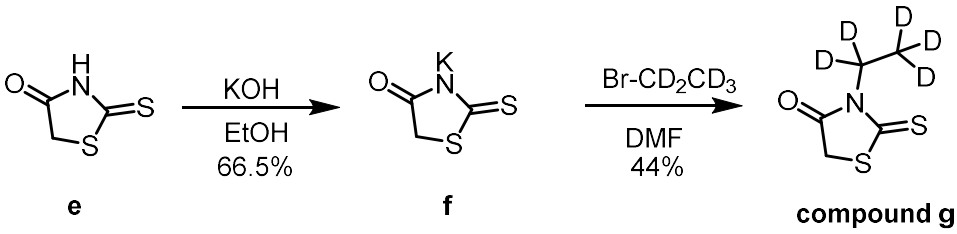

Scheme 5: Synthetic route to deuterated 3-ethyl-d_5-rhodanine

The rhodanine (**e**) was first treated with KOH in order to generate the potassium salt **f** which, in turn, was subjected to an alkylation with bromoethane-d_5 to give the compound **g** with 44% yield.

The synthetic route to the compound **l,** according to the literature procedures,[50] is shown in Scheme 6.

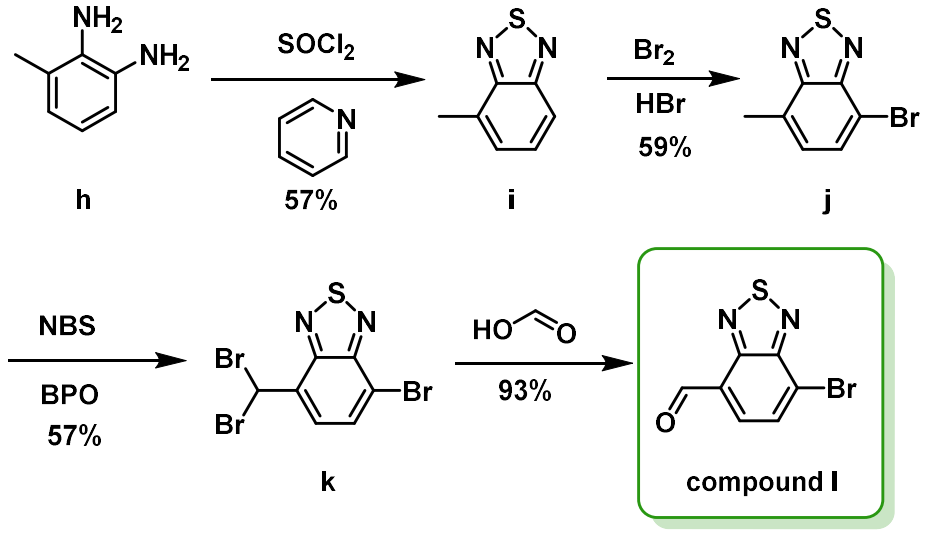

Scheme 6: Synthetic route to compound l

The 3-methylbenzene-1,2-diamine (**h**) was first treated with thionyl chloride in the presence of pyridine in order to perform a cyclization to obtain compound **l**, isolated in 57% yield, which in turn was brominated with bromine and hydrobromic acid to give the compound **j**. Subsequently, the compound **j** was brominated again on the methyl group in the presence of the *N*-bromosuccinimide and benzoyl peroxide to form the dibrominated compound **k** in 57% yield. In the last step compound **k** reacted with the formic acid to give the desired product **l** with a very good yield (93%).

The synthetic route to novel deuterated IDT-BR is shown in Scheme 7.

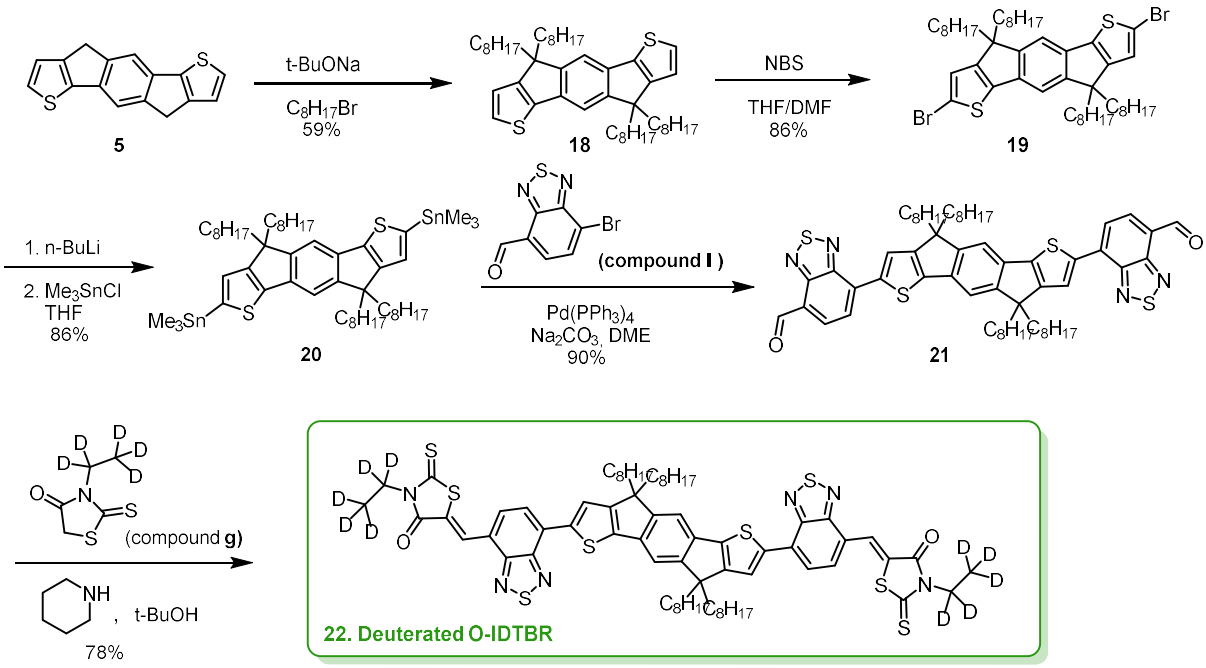

Scheme 7 : Synthetic route to deuterated IDT-BR

IDT (**5**) was used as starting material and was subjected to base treatment with sodium tert-butoxide to give a carbanion which was then treated with 1-bromohexadecane; after chromatographic purification on silica gel, the desired product **18** was obtained with 59% yield. Subsequently, compound **18** was treated with *N*-Bromosuccinimide in THF/DMF to form the dibrominated compound **19** in 86% yield. The brominated indacenodithiophene core was first stannylated with trimethyltin chloride, then reacted via Pd-catalyzed Stille coupling with compound **I**. The last step was the Knoevenagel condensation with the deuterated 3-ethyl-d_5-rhodanine that produced the final product **22** in 78% yield.

4. Conclusions

Since extending the backbone by fusing more aromatic rings in non-fullerene acceptors (NFAs) may further improve the light absorption ability and charge mobility, in my internship work at KAUST I have further extended the 5-ring indacenodithiophene donor unit by incorporating two benzothiophene units to form a novel 9-ring unit. Moreover, I contributed to develop a side-chain engineering on the 5-heterocyclic-ring core (IDT) by introducing an hexadecyl chain as alkyl substituent. This substitution should enhance the solubility, increase the intermolecular π-π stacking interaction and, more importantly, may change the blend morphology, leading to more crystal domains.

In summary, a new non-fullerene polymeric electron acceptor (TBIDT-BT), based on a 9-fused ring with hexadecane alkyl substitutions was synthesized through a multistep procedure in which the last step was a Pd-catalyzed Stille coupling reaction. The properties and uses in devices of this compound will soon be investigated by my research group at KAUST. Due to the enhancement of effective conjugation length, the novel acceptor should show a lower band gap, better planarity and a higher HOMO level. Although the synthesis is reported on a small (laboratory) scale, all of the precursor materials are relatively inexpensive, and the reactions are sufficiently straightforward and characterized by high yields that a larger scale production should be easily possible. This will demonstrate an important advantage in the field of the development of non-fullerene acceptors. To further extend the absorption and increase the driving force, we also designed a new modification of the TBIDT-BT unit endcapping it by two 3-ethylrhodanine units to obtain novel small molecule NFAs (O-TBIDT-BR and EH-TBIDTBR). This synthesis should provide a potential strategy to improve self-assembly behaviour and order degree of the IDT based SMs via increasing dipole moment of the terminal group, which is available to further improve the photovoltaic performance in organic solar cells. Finally, I have carried out a new modification to the molecule previously synthesized by my research group (O-IDTBT)[50] to study its morphological properties. The synthesis of the deuterated molecule IDTBT was therefore completed starting from the modification of 3-ethyl-rodanine in which the CH_2CH_3 groups linked to the two nitrogen's rhodanines were replaced by CD_2CD_3. All the steps in this synthesis provided high yields.

5. Experimental Section

Materials, synthetic procedures, and compounds characterization

All chemicals were purchased from commercial suppliers unless otherwise specified. All reactions were carried out using conventional Schlenk techniques in an inert argon atmosphere. Reactions were monitored by GC/MS and thin layer chromatography (TLC). TLC was performed using 0.25 mm E. Merck silica plates (60F-254), using short-wave UV light as the visualizing agent. Column chromatography was performed using E. Merck silica gel (60, particle size 0.043– 0.063 mm) for flash chromatography (VWR). The ^{1}H NMR and ^{13}C NMR spectra were recorded on BRUKER AV-400, AV-500 and AV-700 spectrometers operating in $CDCl_3$, CD_2Cl_2 or DMSO-d_6 solution at 298 K. The chemical shifts were expressed in δ (ppm) with respect to the TMS and the coupling constants were reported in hertz (Hz). The following abbreviations were used: s (singlet), d (doublet), t (triplet), q (quartet), dd (doublet of a doublet), ddd (doublet of a doublet of a doublet), dt (doublet of triplet), tt (triplet of triplet), m (multiplet) and bs (broad signal) for the characterization of the observed signal multiplicities. Electrospray mass spectrometry was performed with a Thermo Electron Corporation DSQII mass spectrometer. Numeric nomenclature is used to represent the desired compound formed in the synthesis of the new molecule whilst alphabet nomenclature is used to represent the synthesis of the intermediate compounds.

5.1. Synthesis of the IDT unit[52,53]:

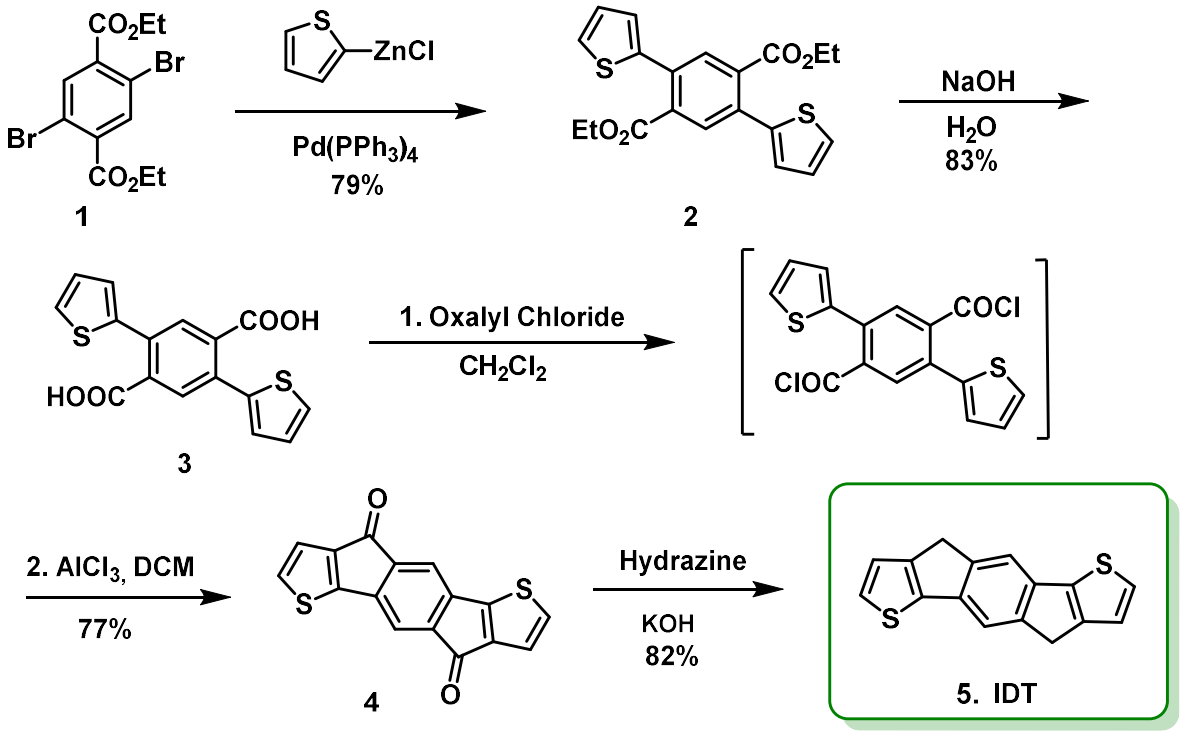

2,5-dithien-2-ylterephthalic acid diethyl ester (2):

A mixture of diethyl 2,5-dibromoterephthalate (**1**) (4.27 g, 11.24 mmol), 2-thienylzinc bromide (0.50 M in anhydrous THF, 50 mL, 25.0 mmol) and $Pd(PPh_3)_4$ (0.39 g, 0.34 mmol) was heated under reflux for 3 hours. After cooled to room temperature, the reaction mixture was poured into saturated NH_4Cl solution. The product was extracted with ethyl acetate for three times. The extracts were combined and washed with water and brine then dried over anhydrous sodium sulfate. After filtration, the solvent was removed under reduced pressure. The residue was purified by column chromatography on silica gel, eluting with n-hexane/ethyl acetate (from 10:0 to 9:1) to obtain the product as pale yellow solid. Yield: 79% (3.43 g).

^1H NMR (400 MHz, $CDCl_3$): δ (ppm) 7.83 (s, 2H, Ar-H), 7.41 (dd, *J* = 4.8 and 1.4 Hz, 2H, Ar-H), 7.10-7.13 (m, 4H, Ar-H), 4.24 (q, *J* = 7.2 Hz, 4H,CH_2), 1.18（t, *J* = 7.2 Hz, 6H, CH_3); ^{13}C NMR (100 MHz, $CDCl_3$): δ (ppm) 167.9, 138.2, 133.7, 133.2, 130.7, 128.6, 128.0, 127.6, 60.9, 14.1.

2,5-dithien-2-ylterephthalic acid (3):

The 2,5-dithien-2-ylterephthalic acid diethyl ester (**2**) (3.20 g, 8.28 mmol) was dissolved in ethanol (200 mL), followed by the addition of a solution of sodium hydroxide (4.50 g NaOH in 30 mL water). This mixture was heated under reflux for 15 hours followed by evaporation under reduced pressure. To the aqueous residue, concentrated hydrochloric acid was added. The precipitate formed was collected by filtration and washed with water then dried in *vacuum* to obtain the product as off-white solid. Yield: 83% (2.27 g).

^{1}H NMR (400 MHz, DMSO-d_6): δ (ppm) 13.48 (s, 2H, COOH), 7.73 (s, 2H, Ar-H), 7.72 (dd, *J* = 5.1 and 1.1 Hz, 2H, Ar-H), 7.30 (dd, *J* = 3.6 and 1.1 Hz, 2H, Ar-H), 7.18 (m, 2H, Ar-H); ^{13}C NMR (100 MHz, DMSO-d_6): δ (ppm) 168.8 (C=O), 139.7 (q), 134.6 (q), 131.5 (q), 130.3 (CH), 127.9 (CH), 127.6 (CH), 127.2 (CH).

4,9-dihydro-s-indaceno[1,2-b:5,6-b']-dithiophene-4,9-dione (4):

The 2,5-dithien-2-ylterephthalic acid (**3**) (2.13 g, 6.45 mmol) was suspended in anhydrous DCM (100 mL), followed by the addition of oxalyl chloride (3.28 g, 25.83 mmol). To this mixture, anhydrous DMF (1.0 mL) was added dropwise at room temperature. The resultant mixture was stirred overnight. The solvent was removed under reduced pressure to afford crude dichloride acid as a yellow solid. The solid obtained was first dissolved in anhydrous DCM (80 mL) then added to a suspension of anhydrous $AlCl_3$ (4.0 g) in DCM (120 mL) at 0°C. The resulting mixture was allowed to warm to room temperature and stirred overnight. After that, the solution was poured into ice-cold HCl solution. The precipitate was collected by filtration and washed with 2 M HCl solution, water and acetone, then dried in *vacuum* to afford a deep blue solid. Yield: 77% (1.46 g).

MS (m/e): 294 (M+, 100%), 281, 266, 207, 193. IR: ν (cm^{-1}) 1705 (C=O). ^{1}H NMR (400 MHz, $CDCl_3$): δ (ppm) 8.84 (s, 2H), 7.56 (dd, 4H, *J* = 1.2, 5.2 Hz); ^{13}C NMR (100 MHz, $CDCl_3$): δ (ppm) 188.2, 149.3, 138.8, 138.3, 137.6, 131.9, 130.7, 121.1.

4,9-dihydro-s-indaceno[1,2-b:5,6-b']-dithiophene, (5, IDT):

A mixture of 4,9-dihydro-s-indaceno-[1,2-b:5,6-b']-dithiophene-4,9-dione (**4**) (1.33 g, 4.52 mmol), hydrazine monohydrate (4.52 g, 90.40 mmol) and KOH (5.07 g, 90.54

mmol) in diethylene glycol (50 mL) was heated at 180ºC for 24 h. The resulting mixture was poured into a beaker that contains ice and hydrochloric acid. Upon the formation of the precipitate, the product was collected by filtration and washed with water and acetone, then dried under *vacuum* to afford the product as pale yellow solid. Yield: 82% (0.98 g).

^{1}H NMR (400 MHz, DMSO-d_6): δ (ppm) 7.73 (s, 2H, Ar-H), 7.56 (d, *J* = 4.8Hz, 2H, Ar-H), 7.22 (d, *J* = 4.8Hz, 2H, Ar-H), 3.79 (s, 4H, CH_2); ^{13}C NMR (100 MHz, $CDCl_3$): δ (ppm) 137.1, 134.9, 133.6, 133.3, 130.8, 126.0, 125.6, 32.0.

5.2. Synthesis of the novel TBIDT-BT polymer

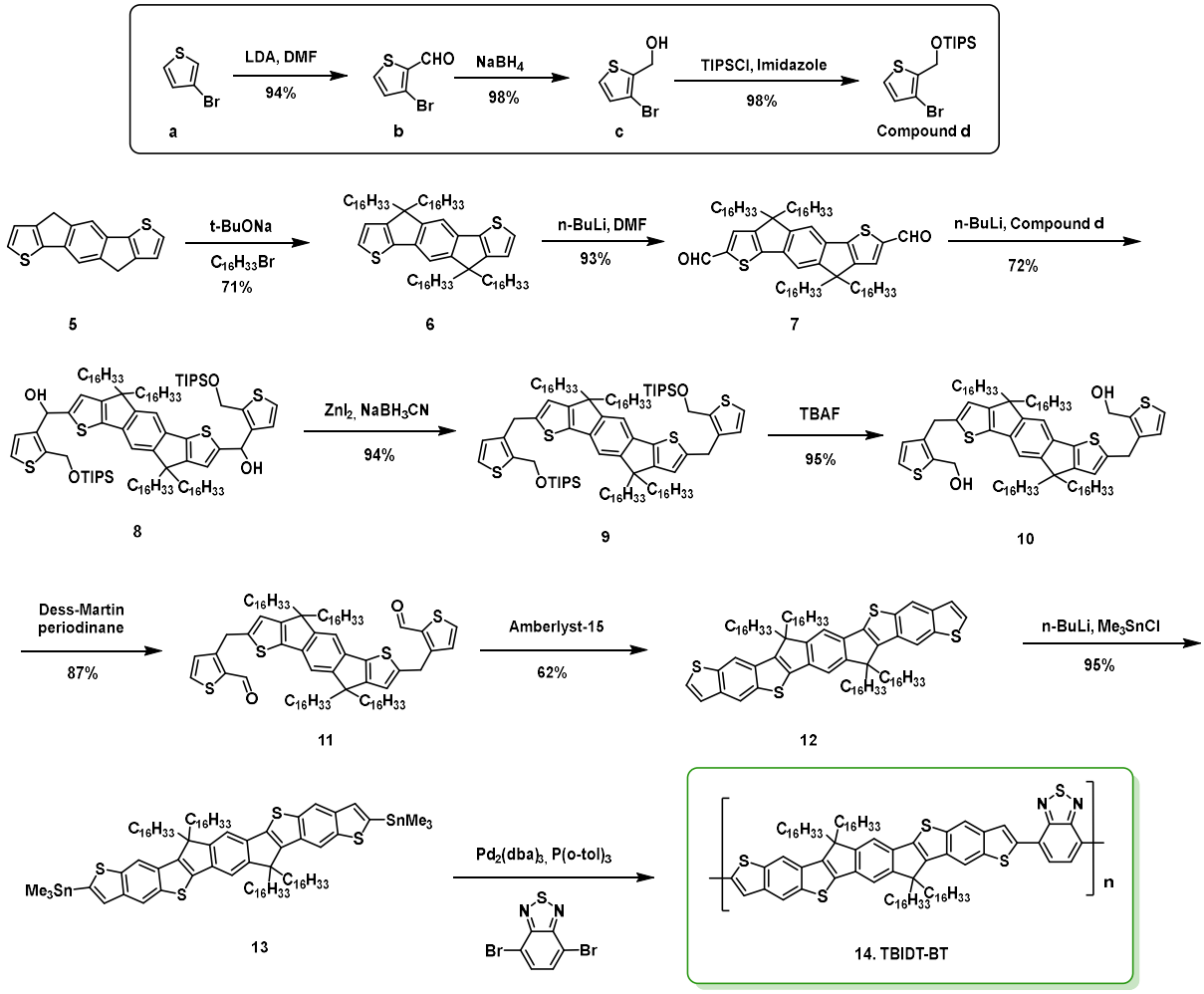

3-bromothiophene-2-carbaldehyde (b):

A solution of LDA in THF (1 M) (67.4 mL, 67.4 mmol) was added dropwise to 3-bromothiophene (**a**) (10 g, 61.3 mmol) in 300 mL of anhydrous THF at 0°C. After stirring the mixture for 1 hour, DMF (5.2 mL, 67.4 mmol) was added to the mixture at 0°C and

the mixture was warmed to room temperature. After stirring for 4 hours, water (100 mL) was added to the mixture and it was extracted with diethyl ether for three times. The organic layers were collected, dried over anhydrous magnesium sulfate, filtered and concentrated under *vacuum*. The product was purified by column chromatography on silica gel with n-hexane/ethyl acetate (50:1) as eluent to give a yellow oil. Yield: 94% (11.0 g).

^{1}H NMR (400 MHz; $CDCl_3$): δ (ppm) 7.15 (d, 1H, *J* = 4.8 Hz), 7.73 (dd, 1H, *J* = 1.2, 5.2 Hz), 9.98 (d, 1H, *J* = 1.2 Hz); ^{13}C NMR (100 MHz; $CDCl_3$): δ (ppm) 183.03, 136.90, 134.87, 132.03, 120.38.

(3-bromothiophen-2-yl) methanol (c):

The 3-bromothiophene-2-carbaldehyde (**b**) (11 g, 57.6 mmol) was dissolved in methanol (300 mL) and cooled to 0°C. Followed by the addition of $NaBH_4$ (3.3 g, 86.4 mmol) in small portions to the mixture and stirred for 4 hours. After that, water (100 mL) was added to the mixture and it was extracted with diethyl ether for three times. The organic phases were collected, dried over anhydrous magnesium sulfate, filtered and concentrated under *vacuum*. The product was purified by column chromatography on silica gel with n-hexane/ethyl acetate (10:1) as eluent to obtain a colourless oil. Yield: 98% (10.9 g).

^{1}H NMR (500 MHz, $CDCl_3$): δ (ppm) 7.28 (d, 1H, *J* = 5.2 Hz), 6.98 (d, 1H, *J* = 5.2 Hz), 4.83 (d, 2H, *J* = 6.4 Hz), 2.98 (s, br, 1H); ^{13}C NMR (176 MHz, $CDCl_3$): δ (ppm) 138.31, 130.13, 125.48, 108.89, 58.96.

((3-bromothiophen-2-yl)methoxy)triisopropylsilane (d):

To a solution of (3-bromothiophen-2-yl)methanol (**c**) (10 g, 51.8 mmol) and triisopropylsilylchloride (11.98 g, 62.16 mmol) in dichloromethane was added the imidazole (8.82 g, 129.5 mmol). The mixture was stirred for 12 hours, diluted with saturated aq. NH_4Cl, extracted with EtOAc, washed with brine and concentrated under *vacuum*. The residue was purified by column chromatography on silica gel with petroleum ether/ethyl acetate (50:1) as eluent to obtain the product as a colorless liquid. Yield: 98% (17.74 g).

^{1}H NMR (500 MHz, $CDCl_3$): δ (ppm) 7.21 (d, *J* = 5.3 Hz, 1H), 6.92 (d, *J* = 5.3 Hz, 1H), 4.92 (s, 2H), 1.22-1.18 (m, 3H), 1.12 (s, 18H); ^{13}C NMR (176 MHz, $CDCl_3$): δ (ppm) 140.83, 129.60, 124.39, 105.30, 61.23, 18.01, 12.01.

4,9-dihydro-4,4,9,9-tetrahexadecyl-s-indaceno[1,2-b:5,6-b']-dithiophene (6):

To a mixture of 4,9-dihydro-s-indaceno[1,2-b:5,6-b']-dithiophene (**5**) (0.92 g, 3.46 mmol) in anhydrous DMSO (20 mL) was added sodium tert-butoxide (1.99 g, 20.73 mmol) in small portions. The reaction mixture was heated at 80ºC for 1 hour, followed by the addition of 1-bromohexadecane (6.33 g, 20.75 mmol) dropwise. Subsequently, the resultant mixture was heated at 80 ºC for 5 hours, then poured into ice-water. The precipitate was collected by filtration and washed with water and methanol to give a black solid. This solid was purified by column chromatography on silica gel with n-hexane as the eluent, to obtain an off-white solid. Yield: 59% (2.38 g).

^{1}H NMR (700 MHz, $CDCl_3$): δ (ppm) 7.29 (s, 2H, Ar-H), 7.27 (d, *J* = 4.8 Hz, 2H, Ar-H), 6.98 (d, *J* = 4.8 Hz, 2H, Ar-H), 1.94-2.04 (m, 4H, CH_2), 1.81-1.92 (m, 4H, CH_2) 1.02-1.46 (m, 104H, CH_2), 0.75-0.98 (m, 20H, CH_2 and CH_3); ^{13}C NMR (100 MHz, $CDCl_3$): δ (ppm) 155.20, 153.22, 141.84, 135.72, 126.25, 121.73, 113.21, 53.85, 39.16, 32.11, 31.96, 30.12, 29.78 29.77, 29.76, 29.75, 29.74, 29.71, 29.43, 29.41, 24.32, 22.81, 22.73, 14.22.

4,4,9,9-tetrahexadecyl-4,9-dihydro-s-indaceno[1,2-b:5,6-b']dithiophene-2,7-dicarbaldehyde (7):

The 4,4,9,9-tetrahexadecyl-4,9-dihydro-s-indaceno[1,2-b:5,6-b']dithiophene (**6**) (10 g, 8.59 mmol) was dissolved in anhydrous THF (100 mL) and cooled to -78°C under argon. The n-butyllithium solution (2.5 M, 8.59 mL) was then added dropwise and the mixture was warmed up to 0°C and stirred for 30 min. The mixture was cooled to -78°C again and 1 mL of DMF was added dropwise into the solution and the mixture was warmed up to room temperature and stirred for an additional 6 hours. Water (100 mL) was added to the mixture and the product was extracted with ethyl acetate for three times. The organic phases were collected, dried over anhydrous magnesium sulfate, filtered and concentrated under *vacuum*. The product was purified by column chromatography on silica gel with n-hexane/ethyl acetate (5:1) as eluent to give a yellow solid. Yield: 93% (9.75 g).

^{1}H NMR (700 MHz, $CDCl_3$): δ (ppm) 9.94 (s, 1H), 7.66 (s, 1H), 7.48 (s, 1H), 2.12-2.10 (m, 8H), 1.36-0.92 (m, 104H), 0.91-0.87 (m, 12H), 0.82-0.65 (m, 8H); ^{13}C NMR (126 MHz, $CDCl_3$): δ (ppm) 182.96, 156.06, 155.18, 151.40, 145.60, 136.47, 130.41, 115.03, 53.81, 39.12, 32.11, 31.96, 30.12, 29.84, 29.77, 29.76, 29.75, 29.74, 29.71, 29.43, 29.41, 24.32, 22.81, 22,73, 14.22.

(4,4,9,9-tetrahexadecyl-4,9-dihydro-s-indaceno[1,2-b:5,6-b']dithiophene-2,7-diyl)bis((2-(((triisopropylsilyl)oxy)methyl)thiophen-3-yl)methanol) (8):

The ((3-bromothiophen-2-yl)methoxy)triisopropylsilane (**d**) (5 g, 14.3 mmol) was dissolved in 100 mL anhydrous diethyl ether and cooled to -78°C. Then, n-butyllithium solution (2.5 M, 5.72 mL) was added dropwise and was stirred for 30 min. The (4,4,9,9-tetrahexadecyl-4,9-dihydro-s-indaceno[1,2-b:5,6-b']dithiophene-2,7-dicarbaldehyde) (**7**) (5.82 g, 4.76 mmol) was then dissolved in 50 mL of anhydrous diethyl ether and was added dropwise into the solution and stirred for further 30 min. The mixture was warmed to room temperature and stirred overnight. After that, water (150 mL) was added to the mixture and the mixture was extracted with ethyl acetate for three times. The organic phases were collected, dried over anhydrous magnesium sulfate, filtered and concentrated under *vacuum*. The product was purified by column chromatography on silica gel with n-hexane/dichloromethane (3:1) as eluent to give a brown liquid. Yield: 72% (6.04 g).

^{1}H NMR (700 MHz, $CDCl_3$): δ (ppm) 7.26 (s, 2H), 7.16 (s, 2H), 7.14 (d, *J* = 5.2 Hz, 2H), 7.03 (d, *J* = 5.2 Hz, 2H), 6.17 (d, *J* = 4.8 Hz, 2H), 4.97 (s, 4H), 2.15-2.10 (m, 8H), 1.23-1.14 (m, 6H), 1.34-0.97 (m, 140H), 0.91-0.82 (m, 12H), 0.81-0.65 (m, 8H); ^{13}C NMR (176 MHz, $CDCl_3$): δ (ppm) 171.19, 154.24, 152.54, 148.90, 145.69, 141.11, 140.71, 139.54, 135.67, 128.11, 126.40, 124.23, 123.09, 122.98, 119.11, 112.79, 60.43, 44.60, 31.96, 29.76, 29.71, 29.41, 22.73, 21.08, 18.03, 18.01, 17.99, 17.73, 14.22, 14.16, 12.02, 11.95.

(((((4,4,9,9-tetrahexadecyl-4,9-dihydro-s-indaceno[1,2-b:5,6-b']dithiophene-2,7-diyl)bis(methylene))bis(thiophene-3,2-diyl))bis(methylene))bis(oxy)) bis(triisopropylsilane) (9):

The ((4,4,9,9-tetrahexadecyl-4,9-dihydro-s-indaceno [1,2-b:5,6-b'] dithiophene-2,7-diyl) bis ((2-(((triisopropylsilyl)oxy)methyl)thiophen-3-yl)methanol)) (**8**) (10.87 g, 6.17

mmol) was dissolved in 100 mL of dichloromethane, followed by the addition of ZnI_2 (0.40 g, 1.24 mmol) in one portion, then $NaBH_3CN$ (1.17 g, 18.52 mmol). The mixture was stirred overnight and then quenched by water (100 mL). The mixture was extracted with ethyl acetate for three times. The organic phases were collected, dried over anhydrous magnesium sulfate, filtered and concentrated under *vacuum*. The product was purified by column chromatography on silica gel with n-hexane as the eluent to give a yellow liquid. Yield: 94% (10.04 g).

^{1}H NMR (700 MHz, $CDCl_3$): δ (ppm) 7.26 (s, 2H), 7.14 (d, *J* = 5.1 Hz, 2H), 6.87 (d, *J* = 5.1 Hz, 2H), 6.65 (s, 2H), 4.96 (s, 4H), 4.14 (s, 4H), 2.15-2.10 (m, 8H), 1.28-1.14 (m, 6H), 1.34-0.96 (m, 140H), 0.91-0.85 (m, 12H), 0.82-0.64 (m, 8H); ^{13}C NMR (176 MHz, $CDCl_3$): δ (ppm) 154.43, 152.29, 145.05, 139.98, 139.90, 135.51, 134.85, 129.04, 126.84, 124.53, 123.09, 121.23, 119.68, 112.50, 59.59, 41.36, 39.07, 36.09, 31.96, 29.75, 27.70, 24.24, 22.73, 20.48, 18.62, 18.03, 17.99, 17.85, 14.22, 14.17, 12.97, 11.48.

(((4,4,9,9-tetrahexadecyl-4,9-dihydro-s-indaceno[1,2-b:5,6-b']dithiophene-2,7-diyl) bis(methylene))bis(thiophene-3,2-diyl))dimethanol (10):

(((((4,4,9,9-tetrahexadecyl-4,9-dihydro-s-indaceno [1,2-b:5,6-b'] dithiophene-2,7-diyl) bis(methylene)) bis(thiophene-3,2-diyl))bis(methylene))bis(oxy)) bis(triisopropylsilane) (**9**) (5.58 g, 3.23 mmol) was first dissolved in anhydrous THF (100 mL) followed by the addition of TBAF (1M in THF, 8.07 mL). The mixture was stirred overnight then quenched by water (100 mL). The mixture was extracted with ethyl acetate for three times and the organic phases were collected, dried over anhydrous magnesium sulfate, filtered and concentrated under *vacuum*. The product was purified by column chromatography on silica gel with n-hexane/dichloromethane (1:1) as the eluent to give a yellow liquid. Yield: 95% (4.35 g).

^{1}H NMR (700 MHz, $CDCl_3$): δ (ppm) 7.26 (s, 2H), 7.21 (d, J = 5.1 Hz, 2H), 6.93 (d, J = 5.1 Hz, 2H), 6.69 (s, 2H), 4.83 (s, 4H), 4.21 (s, 4H), 2.14-2.12 (m, 8H), 1.32-0.97 (m, 104H), 0.91-0.84 (m, 12H), 0.82-0.64 (m, 8H); ^{13}C NMR (176 MHz, $CDCl_3$): δ (ppm) 171.26, 154.54, 152.31, 145.13, 140.06, 137.83, 137.71, 135.49, 129.52, 124.29, 119.71, 112.55, 60.46, 57.78, 53.94, 39.07, 31.96, 30.08, 29.75, 29.71, 29.69, 29.46, 29.41, 24.23, 22.73, 21.09, 17.73, 14.22, 14.17, 12.29.

3,3'-((4,4,9,9-tetrahexadecyl-4,9-dihydro-s-indaceno[1,2-b:5,6-b']dithiophene-2,7-diyl)bis(methylene))bis(thiophene-2-carbaldehyde) (11):

(((4,4,9,9-tetrahexadecyl-4,9-dihydro-s-indaceno [1,2-b:5,6-b'] dithiophene-2,7-diyl) bis(methylene))bis(thiophene-3,2-diyl))dimethanol (**10**) (5.22 g, 3.68 mmol) was dissolved in 100 mL of dichloromethane. The Dess-Martin periodinane (3.91 g, 9.22 mmol) was added into the solution and the mixture was stirred overnight. The resulting mixture was gradually quenched by saturated $NaHCO_3$ solution. The mixture was stirred at room temperature for 30 min and saturated NaS_2SO_3 solution was added. The mixture was extracted with ethyl acetate for three times. The organic phases were collected, dried over anhydrous magnesium sulfate, filtered and concentrated under *vacuum*. The product was purified by column chromatography on silica gel with n-hexane/dichloromethane (1:1) as the eluent to give a yellow solid. Yield: 87% (4.52 g).

^{1}H NMR (700 MHz, $CDCl_3$): δ (ppm) 10.13 (s, 2H), 7.65 (d, J = 5.0 Hz, 2H), 7.14 (s, 2H), 7.05 (d, J = 5.0 Hz, 2H), 6.74 (s, 2H), 4.56 (s, 4H), 2.13-2.11 (m, 8H), 1.36-0.96 (m, 104H), 0.90-0.86 (m, 12H), 0.83-0.69 (m, 8H); ^{13}C NMR (176 MHz, $CDCl_3$): δ (ppm) 182.09, 154.69, 152.44, 149.14, 143.00, 141.50, 140.61, 137.85, 135.50, 134.50, 131.27, 131.08, 128.42, 128.26, 53.93, 39.01, 31.90, 30.25, 29.71, 29.73, 29.63, 29.41, 29.49, 24.22, 22.71, 21.39, 17.43, 14.12, 14.10, 12.49.

TBIDT (12):

3,3'-((4,4,9,9-tetrahexadecyl-4,9-dihydro-s-indaceno[1,2-b:5,6-b']dithiophene-2,7-diyl) bis(methylene))bis(thiophene-2-carbaldehyde) (**11**) (3.77 g, 2.67 mmol) was dissolved in toluene (100 mL) and 5.0 g of Amberlyst-15 was added into the solution. The mixture was refluxed overnight, and the water generated in situ was removed by a Dean-Stark Trap. The mixture was filtered, and the filtrate was concentrated under *vacuum*. The crude product was purified by column chromatography on silica gel with n-hexane as eluent to give a pale yellow solid. Yield: 62% (2.28 g).

^{1}H NMR (700 MHz, CD_2Cl_2): δ (ppm) 8.37 (s, 2H), 8.31 (s, 2H), 7.52 (s, 2H), 7.51 (d, J = 5.3 Hz, 2H), 7.41 (d, J = 5.4 Hz, 2H), 2.13-2.11 (m, 8H), 1.34-0.96 (m, 104H), 0.91-0.86 (m, 12H), 0.82-0.69 (m, 8H); ^{13}C NMR (176 MHz, CD_2Cl_2): δ (ppm) 139.07, 131.37, 127.83, 126.75, 122.52, 122.09, 121.64, 117.43, 111.44, 108.12, 103.46,

99.16, 98.40, 61.37, 60.89, 60.84, 40.43, 24.10, 16.91, 14.67, 14.65, 14.64, 14.61, 14.58, 14.46, 14.35, 14.17, 8.78, 7.68, 0.90.

TBIDT-Me_3Sn (13):

TBIDT (**12**) (3.42 g, 2.49 mmol) was dissolved in 80 mL of anhydrous THF and cooled to -78°C. A solution of n-butyllithium (2.5 M, 2.49 mL) was added dropwise and stirred for 30 min. After that, the Me_3SnCl solution (1 M in THF) (6.23 mL) was added dropwise into the solution and the mixture was warmed up to room temperature and stirred overnight, then quenched by water (80 mL). The mixture was extracted with ethyl acetate for three times. The organic phases were collected, concentrated under *vacuum*. The product was recrystallized in acetonitrile/dichloromethane to afford a pale yellow solid. Yield: 95% (4.02 g).

^1H NMR (500 MHz, CD_2Cl_2): δ (ppm) 8.36 (s, 1H), 8.32 (s, 2H), 7.53 (s, 2H), 7.50 (s, 2H), 2.53-2.34 (m, 4H), 2.34-2.16 (m, 4H), 1.41-0.95 (m, 104 H), 0.93-0.86 (m, 12H), 0.84-0.61 (m, 8H) 0.50 (s, 18H). ^{13}C NMR (176 MHz, $CDCl_3$): δ (ppm) 139.07, 131.37, 126.75, 123.9, 122.52, 122.09, 121.64, 117.43, 111.44, 108.12, 103.46, 99.16, 98.40, 61.37, 60.89, 60.84, 40.43, 24.10, 16.91, 14.67, 14.65, 14.64, 14.61, 14.58, 14.46, 14.35, 14.17, 8.78, 7.68, 0.90. -6.25, -8.04, -9.85.

TBIDT-BT (14):

A 2.5 mL microwave vial was charged with TBIDT-Me_3Sn (**13**) (0.40 g, 0.233 mmol), 4,7-dibromobenzo[c][1,2,5]thiadiazole (0.068 g, 0.233 mmol), 2 mol% of tris (dibenzylideneacetone) dipalladium (2.9 mg, 0.005 mmol) and tri(o-tolyl) phosphine (6 mg, 0.02 mmol). The vial was sealed and chlorobenzene (1 mL) was added. The obtained solution was degassed with argon for 30 minutes. The vial was subjected to the following reaction conditions in the microwave reactor: 2 minutes at 100°C, 2 minutes at 120°C, 5 minutes at 140°C, 5 minutes at 160°C and 20 minutes at 180°C. The polymer was end-capped by addition of 0.1 eq. of 2-bromobenzene before the reaction mixture was resubmitted to the microwave reactor, 1 minute at 100°C, 1 minute at 120°C, 2 minutes at 140°C and 5 minutes at 160°C. The polymeric solution was cooled down and 0.1 eq. of 2-(trimethylstannyl)benzene was added by syringe. The reaction vial was subjected to the previously mentioned temperature scheme to finalize the end-capping reaction. After reaction, the crude polymer was precipitated in

methanol and was further purified by Soxhlet extractions with acetone, n-hexane and chloroform for 24 hours each. Remaining palladium residues were removed by treating a polymeric chloroform solution with an aqueous sodium diethyldithiocarbamate solution for 2 hours at 50°C under vigorous stirring. Afterwards the organic phase was separated from the aqueous phase and washed several times with water. The polymeric solution was concentrated under reduced pressure and the solid was precipitated from cold methanol. The dark blue solid polymer was filtered off and dried under high *vacuum* for 24 hours.

^{1}H NMR (500 MHz, $CDCl_3$): δ (ppm) 8.71 (br, 2H), 8.37 (br, 2H), 8.13 (br, 2H), 7.68 (br, 2H), 7.74 (br, 2H), 2.14-2.10 (br, 8H), 0.95-1.32 (br, 104H), 0.91-0.84 (br, 12H), 0.82-0.61 (br, 8H).

^{1}H and ^{13}C NMR spectra for TBIDT in CD_2Cl_2:

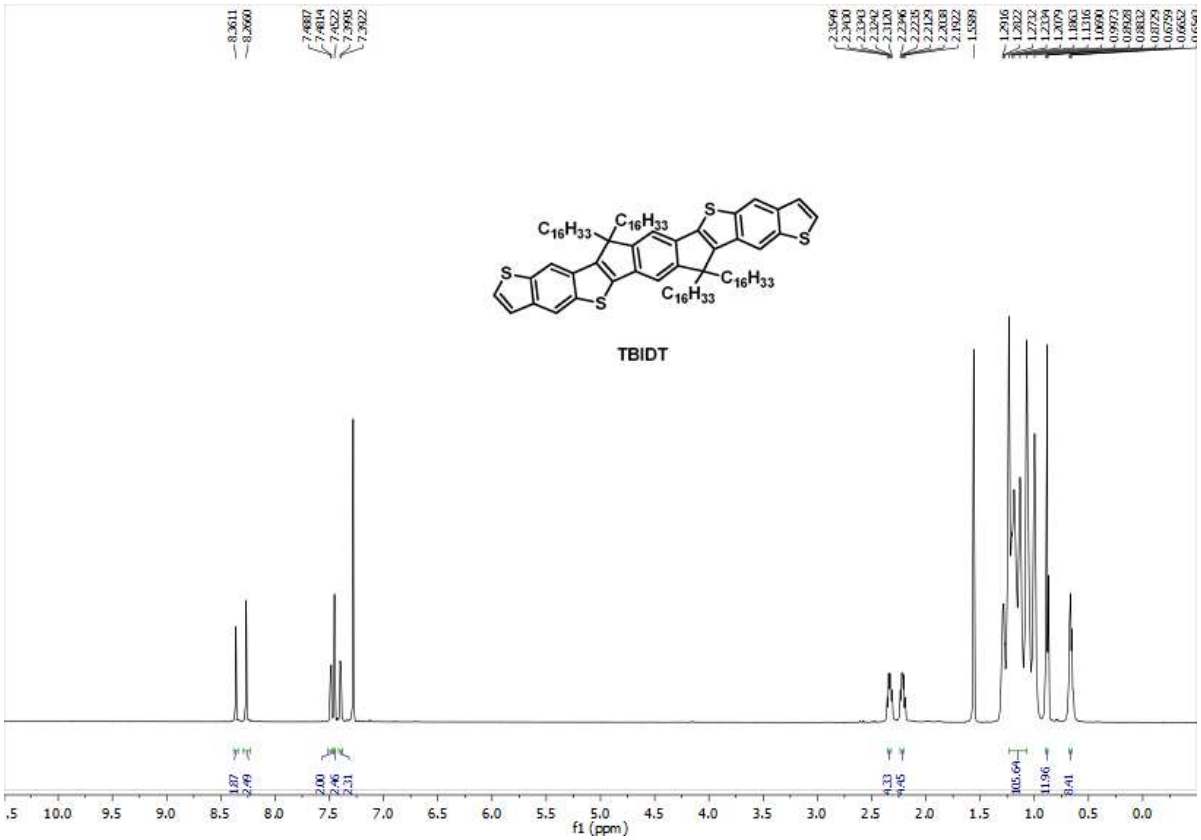

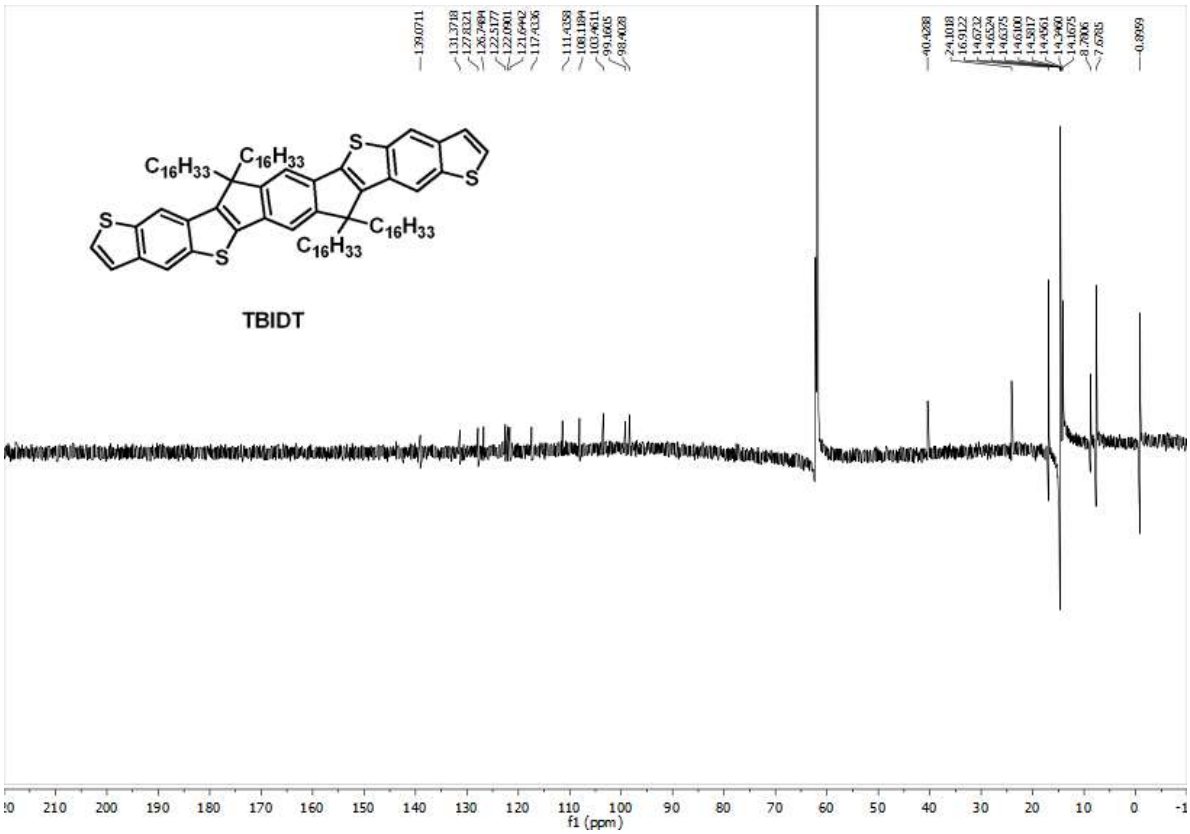

5.3. Synthesis of the non-fullerene IDT-based small molecules O-TBIDTBR and EH-TBIDTBR as novel acceptors, alkylated with linear (n-octyl)- branched (2-ethylhexyl)- side chains:

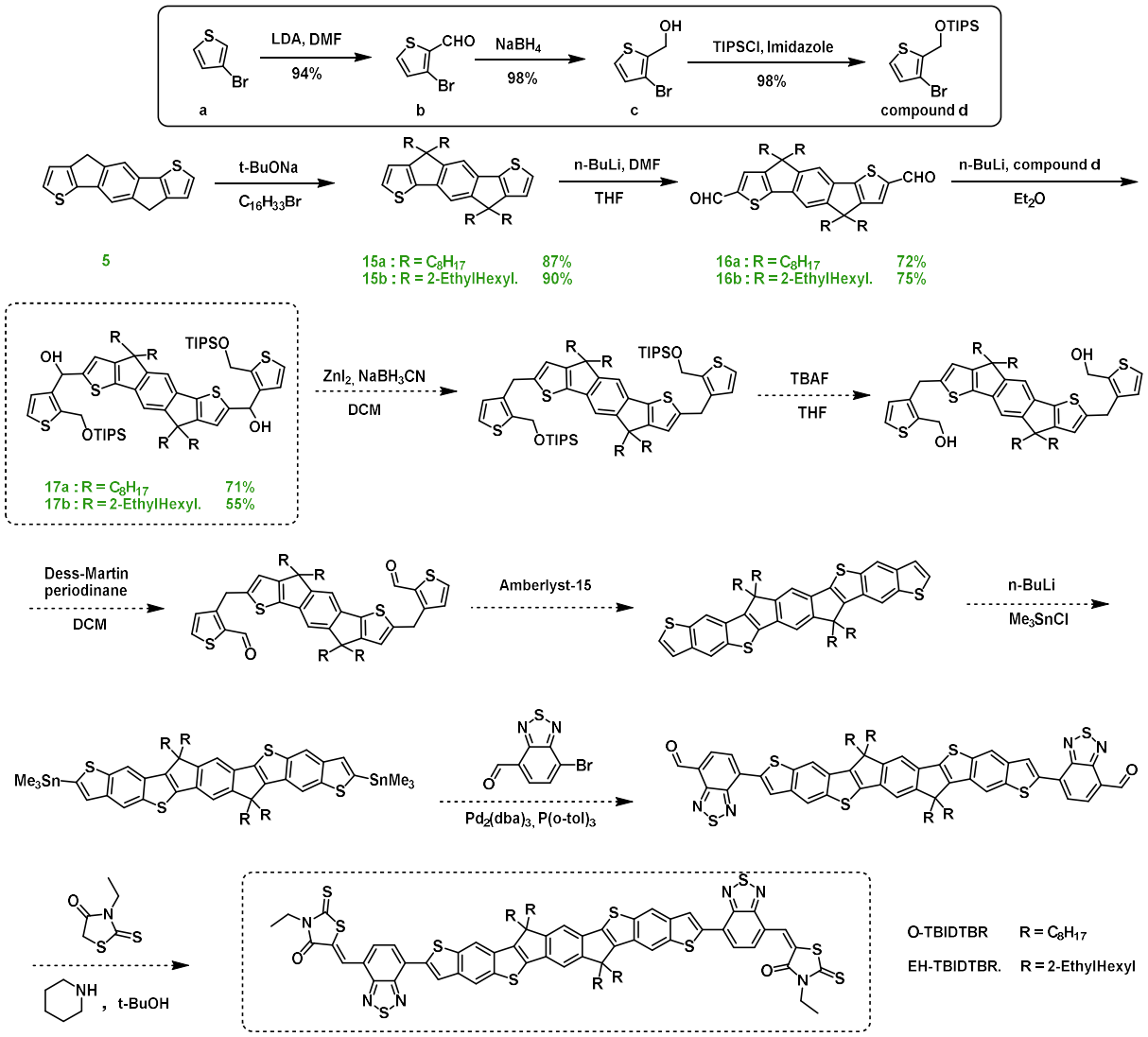

Procedure reported in section 5.2. was used for the synthesis of compounds 17a and 17b.

5.4. Synthesis of a novel deuterated IDT-BR for future morphology studies:

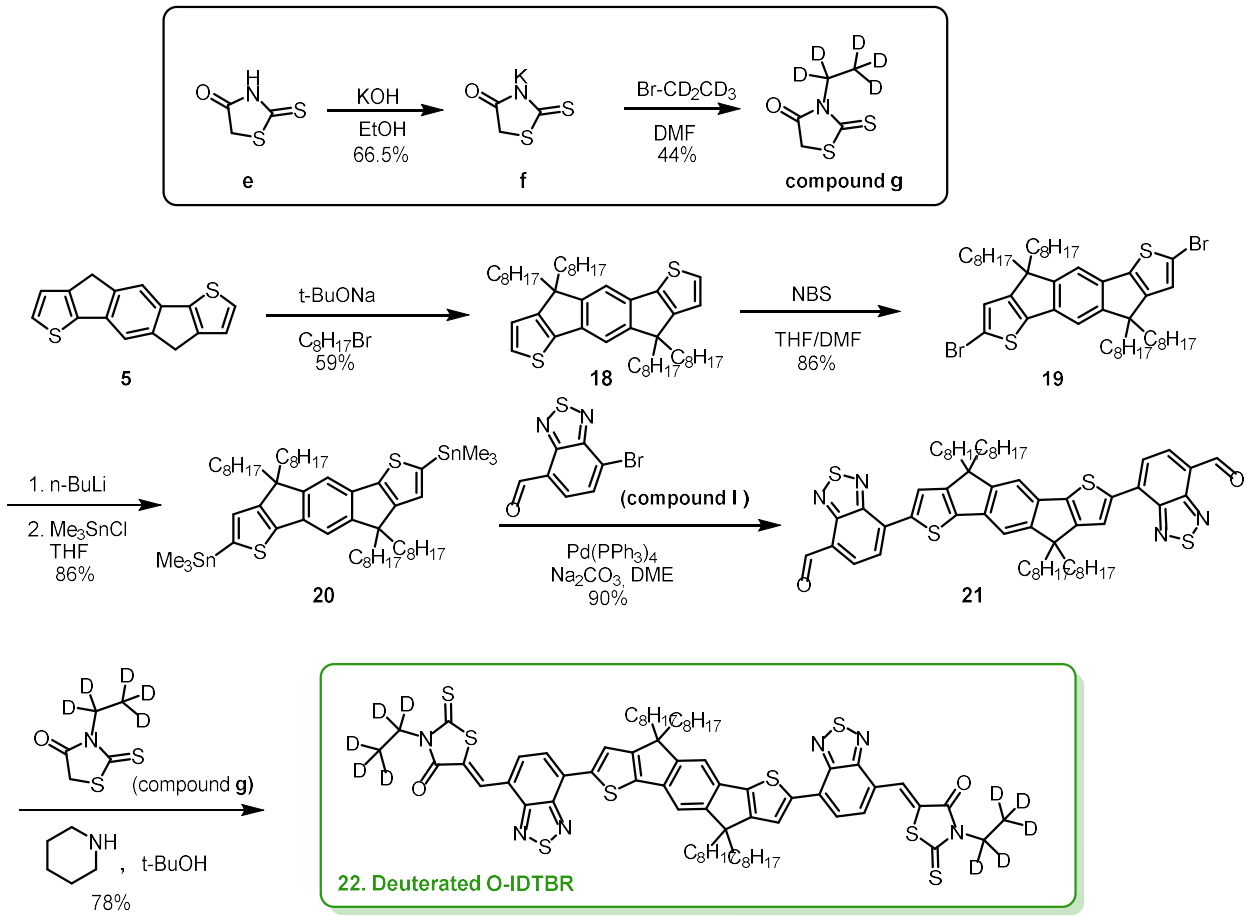

Synthesis of 3-rhodanine-K (f):

KOH (14.02 g, 0.25 mol) was first dissolved in ethanol (50 mL) and it was added dropwise into the solution of 3-H-rhodanine (**e**) (26.64 g, 0.20 mol) that was dissolved in hot ethanol (50 mL) at 80ºC. The mixture was stirred at 80ºC for 2 hours and then cooled in an ice-bath. The crystalline solid was collected on a filter paper, washed with ethanol and air-dried. The potassium salt of rhodanine was obtained. Yield 66.5% (22.75 g). This product was directly used for next step without purification and characterization.

Synthesis of 3-rhodanine-CD_2CD_3 (g):

The $BrCD_2CD_3$ (1.01 mL, 0.014 mol) was added slowly to a suspension of the above potassium salt, 3-rhodanine-K (**f**) (2.0 g, 0.0117 mol) in DMF (10 mL). Upon completion of the addition, the mixture was stirred and heated under reflux at 100ºC for 4 hours. The reaction mixture was then poured into water. Then the mixture was extracted by

CH_2Cl_2 and washed by water, the organic phase was dried by anhydrous Na_2SO_4, filtered, concentrated and purified by column chromatography on silica gel, to get bright yellow liquid 3-rhodanine-CD_2CD_3. Yield: 44% (0.83 g).

^{1}H NMR (500 MHz, $CDCl_3$): δ (ppm) 3.96 (2H, s); ^{13}C NMR (100 MHz, $CDCl_3$): δ (ppm) ($J_{C\text{-}D}$ not reported): 201.05, 173.63, 39.84, 35.49, 11.97

4,4,9,9-tetraoctyl-4,9-dihydro-s-indaceno[1,2-b:5,6-b']dithiophene (18):

To a suspension of 4,9-dihydro-s-indaceno[1,2-b:5,6-b']-dithiophene (**5**) (0.92 g, 3.46 mmol) in anhydrous DMSO (20 mL), sodium tert-butoxide (1.99 g, 20.73 mmol) was added in parts. The reaction mixture was heated at 80ºC for 1 hour, followed by the addition of 1-bromooctane (20.75 mmol) dropwise. After the addition, the resultant mixture was heated at 90ºC for 5 hours, then poured into ice-water. The precipitate was collected by filtration and washed with water and methanol to give a black solid. This was purified by column chromatography on silica gel, eluting with n-hexane, to give a pale yellow solid. Yield: 59% (1.46 g).

^{1}H NMR (400 MHz, $CDCl_3$): δ (ppm) 7.28 (s, 2H, Ar-H), 7.21 (d, J = 4.6, 2H, Ar-H), 6.96 (d, J = 4.5, 2H, Ar-H), 2.00-1.87 (m, 8H, Alkyl-H), 1.30-1.00 (m, 48H, Alkyl-H), 0.88-0.73 (m, 12H, Alkyl-H). ^{13}C NMR (100 MHz, $CDCl_3$): δ (ppm) 154.0, 152.1, 141.9, 135.5, 126.6, 124.8, 113.0, 54.7, 39.0, 31.8, 30.0, 29.7, 29.3, 24.1, 22.6, 14.1.

2,7-dibromo-4,4,9,9-tetraoctyl-4,9-dihydro-s-indaceno[1,2-b:5,6-b']dithiophene (19):

To a solution of 4,4,9,9-tetraoctyl-4,9-dihydro-s-indaceno[1,2-b:5,6-b']dithiophene (**18**) (1.86 mmol) in anhydrous THF/DMF (2:1, 100 mL), N-bromosuccinimide (4.10 mmol) was added. This mixture was stirred for 3 hours at room temperature in the absence of light, then poured into water. The precipitate was collected and washed with water then recrystallized with acetone, to give product as pale yellow solid. Yield: 86% (1.40 g).

^{1}H NMR (400 MHz, $CDCl_3$): δ (ppm) 7.17 (s, 2H), 6.97 (s, 2H), 1.98-1.75 (m, 8H), 1.31-1.00 (m, 48H), 0.86-0.78 (m, 12H). ^{13}C NMR (100 MHz, $CDCl_3$): δ (ppm) 154.0, 152.1, 141.9, 135.5, 124.8, 113.0, 112.4, 54.7, 39.0, 31.8, 30.0, 29.7, 29.3, 24.1, 22.6, 14.1.

(4,4,9,9-tetraoctyl-4,9-dihydro-s-indaceno[1,2-b-5,6-b']dithiophene-2,7-diyl)bis(trimethylstannane) (20):

A solution of 2,7-dibromo-4,4,9,9-tetraoctyl-4,9-dihydro-s-indaceno[1,2-b:5,6-b']dithiophene (**19**) (2.11 g, 2.42 mmol) in anhydrous THF (200 mL) was stirred at -78°C for 30 min. Then, the n-BuLi (2.42 mL, 6.04 mmol, 2.5 M in n-hexane) was added dropwise and the solution was stirred at -78°C for 30 min followed by 0°C for 30 min. After cooling again to -78°C, trimethyltin-chloride was added (7.26 mL, 7.56 mmol, 1M in n-hexane) and the solution was allowed to return to room temperature overnight. The reaction was then poured into water and extracted with n-hexane, washed successively with acetonitrile to remove excess trimethyltin-chloride and dried over anhydrous magnesium sulfate to obtain the product as a yellowish oil. Yield: 86% (2.18 g).

MS (ES-ToF): *m/z* calculated for $C_{54}H_{90}S_2Sn$: 1,040.45; *m/z* found 1,041.40 $(M + H)^+$. ^1H NMR (400 MHz, $CDCl_3$): δ (ppm) 7.25 (s, 2H), 6.97 (s, 2H), 1.97-1.91 (m, 4H), 1.86-1.78 (m, 4H), 1.23-1.05 (m, 48H), 0.83-0.80 (t, 12H, J=7Hz), 0.39 (s, 18H); ^{13}C NMR (100 MHz, $CDCl_3$): δ (ppm) 157.15, 153.47, 147.71, 139.24, 135.31, 129.55, 113.42, 53.06, 39.20, 31.87, 30.07, 30.03, 29.31, 24.17, 22.68, 14.14, -6.23, -8.02, -9.83.

7,7'-(4,4,9,9-tetraoctyl-4,9-dihydro-s-indaceno[1,2-b-5,6-b']dithiophene-2,7-diyl)bis(benzo[c][1,2,5]thiadiazole-4-carbaldehyde) (21):

The solution of (4,4,9,9-tetrapctyl-4,9-dihydro-s-indaceno[1,2-b-5,6-b']dithiophene-2,7-diyl)bis(trimethylstannane) (**20**) (1.04 g, 1.0 mmol) and 2,1,3-benzothiadiazole-4-carboxaldehyde (0.73 g, 3.0 mmol) in anhydrous toluene (40 mL) was degassed for 45 min before adding $Pd(PPh_3)_4$ (58 mg, 0.05 mmol). This solution was heated at 100°C overnight. The reaction mixture was then cooled and purified by flash column chromatography on silica mixed with potassium fluoride using $CHCl_3$ as the eluent. Further purification by column chromatography on silica gel using CH_2Cl_2/pentane (1:1) followed by precipitation from methanol to obtain the product as a dark purple solid. Yield: 90% (0.93 g).

MS (ES-ToF): *m/z* calculated for $C_{62}H_{78}N_4O_2S_4$: 1,038.5; *m/z* found 1,041.40. ^1H NMR (400 MHz, $CDCl_3$): δ (ppm) 10.72 (s, 2H), 8.27 (s, 2H), 8.25 (d, *J* = 7.7 Hz, 2H), 8.06 (d, *J* = 7.5 Hz, 2H), 7.45 (s, 2H), 2.05 (dtd, *J* = 59.3, 12.9, 4.6 Hz, 8H), 1.05-1.2 (m,

38H), 0.99-0.81 (m, 10H), 0.77 (t, *J* = 6.8 Hz, 12H); ^{13}C NMR (100 MHz, $CDCl_3$): δ (ppm) 188.44, 157.04, 154.02, 152.29, 147.00, 140.67, 136.44, 134.14, 132.87, 131.62, 124.87, 124.80, 122.80, 114.12, 54.43, 39.16, 31.79, 29.98, 29.29, 29.20, 24.29, 22.58, 14.04.

Deuterated O-IDTBR (22):

7,7'-(4,4,9,9-tetraoctyl-4,9-dihydro-s-indaceno[1,2-b-5,6-b']dithiophene-2,7-diyl)bis(benzo[c][1,2,5]thiadiazole-4-carbaldehyde) (**21**) (0.39 mmol) and 3-rhodanine-CD_2CD_3 (1.16 mmol) were dissolved in tert-butyl alcohol (30 mL). Two drops of piperidine were added and the solution was left to stir at 85ºC overnight. The product was extracted with $CHCl_3$ and dried over anhydrous magnesium sulfate. The crude product was purified by flash column chromatography on silica gel in CH_2Cl_2 and precipitated from methanol. The precipitate was collected and dried by *vacuum* filtration to afford deuterated O-IDTBR as a dark blue solid. Yield: 78% (0.41 g).

^{1}H NMR (400 MHz, DCM-d_2): δ (ppm) 8.41 (s, 2H), 8.18 (s, 2H), 7.98 (d, *J* = 8.0 Hz, 2H), 7,68 (d, *J* = 7.9 Hz, 2H), 7.42 (s, 2H), 2.26-2.02 (m, 8H), 1.25-1.07 (m, 40H), 0.99-0.87 (m, 8H), 0.76 (m, 12H); ^{13}C NMR (100 MHz, $CDCl_3$): δ (ppm) 192.1, 166.11, 157.04, 154.02, 152.29, 147.00, 143.33, 140.67, 136.44, 134.14, 132.87, 131.62, 128.12, 124.87, 124.80, 122.80, 116.00, 114.12, 54.43, 39.16, 31.79, 29.98, 29.29, 29.20, 24.29, 22.58, 14.04, 9.80.

5.4.1. Synthesis of the 7-Bromo-2,1,3-benzothiadiazole-4-carboxaldehyde[50]:

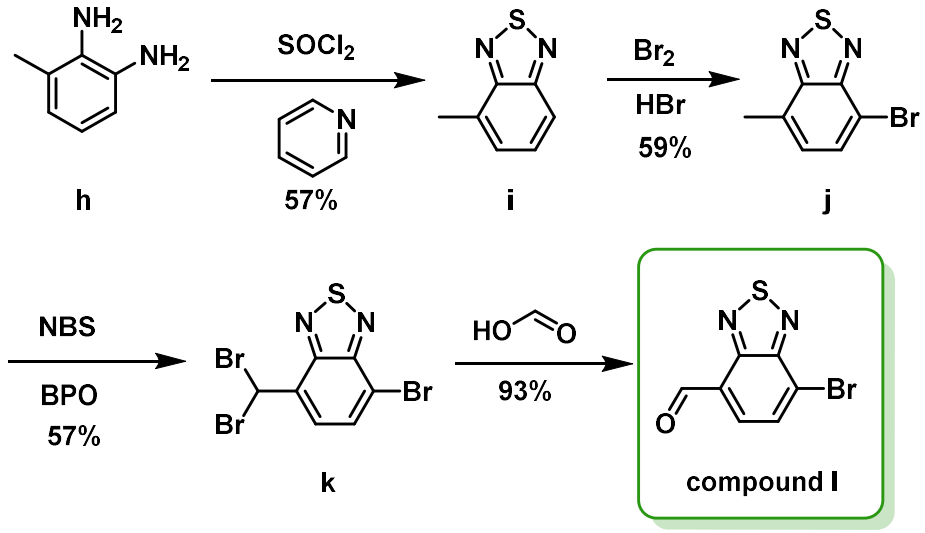

4-methyl-2,1,3-benzothiadiazole (i):

$SOCl_2$ (1.64 mL, 240 mol) was added drop-wise to a solution of 3-methylbenzene-1,2-diamine (**h**) (12 g, 98 mmol) in pyridine (72 mL) with the temperature maintained below 30°C. HCl (48 mL) was then added drop-wise at the temperature maintained below 65°C and the reaction was stirred at room temperature overnight. The reaction mixture was quenched with water and extracted with diethyl ether. After removal of the solvent, the crude product was then purified by steam distillation to obtain a colourless oil. Yield: 57% (8.4 g).

^{1}H NMR (400 MHz, $CDCl_3$): δ (ppm) 7.82 (d, *J* = 8.8 Hz, 1H), 7.47 (dd, *J* = 8.9, 6.7 Hz, 1H), 7.33 (dt, *J* = 6.6, 1.4 Hz, 1H), 2.74 (s, 3H). ^{13}C NMR (100 MHz, $CDCl_3$): δ (ppm) 155.9, 155.2, 130.8, 129.9, 129.7, 118.9, 15.8.

4-bromo-7-methyl-2,1,3-benzothiadiazole (j):

Bromine (2.46 mL, 48 mmol) was added slowly to a solution of 4-methyl-2,1,3-benzothiadiazole (**i**) (7.2 g, 48 mmol) in 50 mL HBr (47% aq). The reaction mixture was heated to 80°C for 30 min after which a solid had precipitated; heating of the solution at 130°C was then continued overnight. The reaction was neutralized with Na_2SO_3 solution, extracted with CH_2Cl_2 and dried over $MgSO_4$ to give the product as a pale yellow solid. Yield: 59% (6.5 g).

^{1}H NMR (400 MHz, $CDCl_3$): δ (ppm) 7.73 (d, *J* = 7.4 Hz, 1H), 7.27 (d, *J* = 7.0 Hz, 1 H), 2.70 (s, 3H). ^{13}C NMR (100 MHz, $CDCl_3$): δ (ppm) 158.4, 158.1, 132.2, 131.9, 129.8, 113.2, 15.8.

4-bromo-7-dibromomethyl-2,1,3-benzothiadiazole (k):

A mixture of 4-bromo-7-methyl-2,1,3-benzothiadiazole (**j**) (5.5 g, 24 mmol), N-bromosuccinimide (12.8 g, 72 mmol) and benzoyl-peroxide (1.16 g, 4.8 mmol) were dissolved in chlorobenzene (50 mL) and stirred overnight at 80°C. After cooling to room temperature, the succinimide precipitate was removed by filtration and water was added to the filtrate which was then extracted with CH_2Cl_2 and dried over anhydrous $MgSO_4$. The crude product was purified by column chromatography on silica gel with n-hexane/CH_2Cl_2 (9:1) as the eluent followed by recrystallization from EtOH afforded the product as a white crystalline solid. Yield: 57% (5.3 g).

^{1}H NMR (400 MHz, $CDCl_3$): δ (ppm) 7.97-7.91 (m, 2H), 7.41 (s, 1H). ^{13}C NMR (100 MHz, $CDCl_3$): δ (ppm) 158.8, 158.1, 116.4, 132.6, 131.9, 130.1, 34.9.

7-bromo-2,1,3-benzothiadiazole-4-carboxaldehyde (l):

A solution of 4-bromo-7-dibromomethyl-2,1,3-benzothiadiazole (**k**) (3 g, 7.8 mmol) in 95% formic acid (30 mL) was refluxed at 110°C for 2 hours, then cooled to room temperature and poured into water. The resulting precipitate was filtered and washed with water until the filtrate was neutral pH. The precipitate was then dried to give an off-white crystalline solid. Yield: 93% (1.75 g).

^{1}H NMR (400 MHz, $CDCl_3$): δ (ppm) 10.74 (s, 1H), 8.09 (s, 1H, *J* = 7.7 Hz), 8.06 (d, 1H, 7.6 Hz). ^{13}C NMR (100 MHz, $CDCl_3$): δ (ppm) 192.0, 159.0, 158.6, 132.8, 132.4, 128.8, 122.0.

6. References

1 BP Statistical Review of Energy 2018, 67th ed. Available online: https://www.bp.com/content/dam/bp/en/corporate/pdf/energy-economics/statistical-review/bp-stats-review-2018-full-report. (Last accessed Jun 13, 2018)

2 S. Manish, I.R. Pillai, R. Banerjee, *Energy Sustain. Dev*., **2006**, *10*, 25-36.

3 P. Tafarte, M. Eichhorn, D. Thrän, *Energies*, **2019**, *12*, 324, doi: 10.3390-en12020324.

4 B. Zaidi, Introduction to Photovoltaic Effect in Solar Panels and Photovoltaic Materials; InTech Open: London, UK, **2018**, pp. 1-8.

5 J.A.L. Sánchez, A.M.D. Pascual, R.P. Capilla, *Int. J. Mol. Sci*., **2019**, *20*, 976, doi: 10.3390/ijms20040976

6 K.D.G.I. Jayawardena, L.J. Rozanski, C.A. Mills, M.J. Beliatis, N.A. Nismy, S.R.P. Silva, *Nanoscale*, **2013**, *5*, 8411-8427.

7 M.A. Green, *Prog. Photovoltaics*, **2001**, *9*, 123-135.

8 G. Conibeer, *Mater. Today*, **2007**, *10*, 42-50.

9 J. Luther, M. Nast, M.N. Fisch, D. Christoffers, F. Pfisterer, D. Meissner, J. Nitsch, M. Becker, *Solar Technology.* **2012**, doi:10.1002/14356007.a24_369.pub2.Wiley-VCH.

10 M. Jørgensen, K. Norrman, F.C. Krebs*, Sol. Energy Mater. Sol. Cells*, **2008**, *92*, 686-714.

11 R. Po, C. Carbonera, A. Bernardi, F. Tinti, N. Camaioni, *Sol. Energy Mater. Sol. Cells*, **2012**, *100*, 97-114.

12 M. C. Scharber, D. Mühlbacher, M. Koppe, P. Denk, C. Waldauf, A.J. Heeger, C.J. Brabec, *Adv. Mater*., **2006**, *18*, 789-794.

13 J. You, L. Dou, K. Yoshimura, T. Kato, K. Ohya, T. Moriarty, K. Emery, C.C. Chen, *Nat. Commun.*, **2013**, *4*, 1446.

14 C. Yongsheng, C. Yong, Y. Hin-Lap, X. Ruoxi, D. Liming, X. Zuo, K. Xin, W. Yanbo, Z. Xin, *Science*, **2018**, *361*, 1094-1098.

15 H. Hoppe, N. S. Sariciftci, *J. Mater. Res. Technol.*, **2004**, 19, 1924-1945.

16 C. W. Tang, *Appl. Phys. Lett.*, **1986**, 48, 183-185.

17 G. Yu, J. Gao, J.C. Hummelen, F. Wudl, A. J. Heeger, *Science*, **1995**, *270*, 1789-1791.

18 H.S. Son, F. He, B. Carsten, *J. Mater. Chem*., **2011**, *21*, 18934-18945.

19 D.G. McGehee, M.A. Topinka, *Nat. Mater.*, **2006**, *5*, 675-676.

20 J. Nelson, *Mater. Today*, **2002**, *5*, 87-95.

21 W. Cao, J. Xue, *Energy Environ. Sci.*, **2014**, *7*, 2123-2144.

22 J.S. Wu, S.W. Cheng, Y.J. Cheng and C.S. Hsu, *Chem. Soc. Rev.*, **2015**, *44*, 1113–1154.

23 L. Ye, S. Zhang, L. Huo, M. Zhang, J. Hou, *Acc. Chem. Res.*, **2014**, *47*, 1595–1603.

24 W. Jiang, Y. Li, Z. Wang, *Acc. Chem. Res.*, **2014**, *47*, 3135–3147.

25 I. McCulloch, R.S. Ashraf, L. Biniek, H. Bronstein, C. Combe, J.E. Donaghey, D.I. James, C.B. Nielsen, B.C. Schroeder, W. Zhang, *Acc. Chem. Res.*, **2012**, *45*, 714-722.

26 L. Ting, C. Yue, F. Yunlong, L. Chen-Jiang, Y. Si-Chun, P. Jian, *J. Am. Chem. Soc.*, **2011**, *133*, 6099-6101.

27 Y. Lin, X. Zhan, *Mater. Horiz.*, **2014**, *1*, 470-488.

28 P.M. Beaujuge, C. M. Amb, J. R. Reynolds, *Acc. Chem. Res.*, **2010**, *43*, 1396-1407.

29 Y. Li, C.-Y. Chang, Y. Chen, Y. Song, C.-Z. Li, H.-L. Yip, A.K.Y. Jen, C. Li, *J. Mater. Chem. C,* **2013**, *1*, 7526-7533.

30 Y. Li, Z. Pan, Y. Fu, Y. Chen, Z. Xie, B. Zhang, *Polym. Chem.*, **2012**, *50*, 1663-1671.

31 E. Havinga, W.T. Hoeve, H. Wynberg, *Polym. Bull.*, **1992**, *29*, 119-126.

32 J.C. Hummelen, B.W. Knight, F. Lepeq, F. Wudl, J. Yao, C.L. Wilkins, *J. Org. Chem.*, **1995**, *60*, 532-538.

[33] Y. Li, K. Yao, H.-L. Yip, F.-Z. Ding, Y.-X. Xu, X. Li, Y. Chen, A.K.Y. Jen, *Adv. Funct. Mater.*, **2014**, *24*, 3631-3638.

[34] Y. Zhang, J. Zou, H.-L. Yip, K.-S. Chen, D.F. Zeigler, Y. Sun, A.K.Y. Jen, *Chem. Mater.*, **2011**, *23*, 2289–2291.

[35] R.S. Ashraf, Z. Chen, S.L. Dong, H. Bronstein, W. Zhang, B. Schroeder, Y. Geerts, J. Smith, S. Watkins, T.D. Anthopoulos, *Chem. Mater.*, **2011**, *23*, 768–770.

36 X. Zhang, H. Bronstein, A. J. Kronemeijer, J. Smith, Y. Kim, R. J. Kline, L.J. Richter, T.D. Anthopoulos, H. Sirringhaus, K. Song, M. Heeney, W. Zhang, I. McCulloch, D.M. DeLongchamp*, Nat. Commun.,* **2013**, *4*, 2238-2246.

37 D. Venkateshvaran, M. Nikolka, A. Sadhanala, V. Lemaur, M. Zelazny, M. Kepa, M. Hurhangee, A. J. Kronemeijer, V. Pecunia, I. Nasrallah, *Nature*, **2014**, *515*, 384-388.

38 Y.X. Xu, C.C. Chueh, H.L. Yip, F.Z. Ding, Y. X. Li, C. Z. Li, X. Li, W. C. Chen, A. K. Y. Jen, *Adv. Mater*., **2012**, *24*, 6356-6361.

39 Y. Sun, S.-C. Chien, H.-L. Yip, Y. Zhang, K.-S. Chen, D. F. Zeigler, F.-C. Chen, B. Lin, A. K. Y. Jen, *J. Mater. Chem*., **2011**, *21*, 13247-13255.

40 C. Y. Yu, C. P. Chen, S. H. Chan, G. W. Hwang, C. Ting, *Chem. Mater*., **2009**, *21*, 3262-3269.

41 Y. Lin, Z. G. Zhang, H. Bai, J. Wang, Y. Yao, Y. Li, D. Zhu, X. Zhan, *Energy Environ. Sci*., **2015**, *8*, 610-616.

42 T. C. Parker, D. G. Patel, K. Moudgil, S. Barlow, C. Risko, J. L. Br´edas, J. R. Reynolds, S. R. Marder, *Mater. Horiz.,* **2015**, *2*, 22-36.

43 Y. C. Chen, C. Y. Yu, Y.L. Fan, L. I. Hung, C. P. Chen, C. Ting, *Chem. Commun*., **2010**, *46*, 6503-6505.

44 Y. Li, M. Gu, Z. Pan, B. Zhang, X. Yang, J. Gu, Y. Chen, *J. Mater. Chem*., **2017**, *5*, 10798-10798.

45 A. Raja Shahid, B. C. Schroeder, H. A. Bronstein, H. Zhenggang, T. Stuart, K. R. Joseph, C. J. Brabec, R. Patrice, T. D. Anthopoulos, J. R. Durrant, *Adv. Mater*., **2013**, *25*, 2029-2034.

46 Z. Fei, R. S. Ashraf, Z. Huang, J. Smith, R. J. Kline, P. D'Angelo, T. D. Anthopoulos, J. R. Durrant, I. McCulloch, M. Heeney, *Chem. Commun*., **2012**, *48*, 2955-2957.

47 B. C. Schroeder, R. S. Ashraf, S. Thomas, A. J. White, L. Biniek, C. B. Nielsen, W. Zhang, Z. Huang, P. S. Tuladhar, S. E. Watkins, *Chem. Commun*., **2012**, *48*, 7699-7701.

48 C. Schwarz, H. B¨assler, I. Bauer, J.-M. Koenen, E. Preis, U. Scherf, A. K¨ohler, *Adv. Mater*., **2012**, *24*, 922-925.

49 J. Roncali, *Macromol. Rapid Commun.,* **2007**, *28*, 1761-1775.

[50] S. Holliday, R. S. Ashraf, C. B. Nielsen, M. Kirkus, J. A. Rohr, C. H. Tan, E. C. Fregoso, A. C. Knall, J. R. Durrant, J. Nelson, I. McCulloch. *J. Am. Chem. Soc*. **2015**, *137*, 898-904.

[51] H. Bronstein, D. S. Lemm, P. Woebkenberg, S. King, W. Zhang, R. S. Ashraf, M. Heeney, T. D. Anthopoulos, J. de Mello and I. McCulloch; *Macromolecules*, **2011,** 44, 17, 6649-6652.

[52] W. Zhang, J. Smith, S. E. Watkins, R. Gysel, M. McGehee, A. Saello, J. Kirkpatrick, S. Ashraf, T. D. Anthopoulos, M. Heeney, and I. McCulloch; *J. Am. Chem. Soc*. **2010**, *132*, 11437-11439.